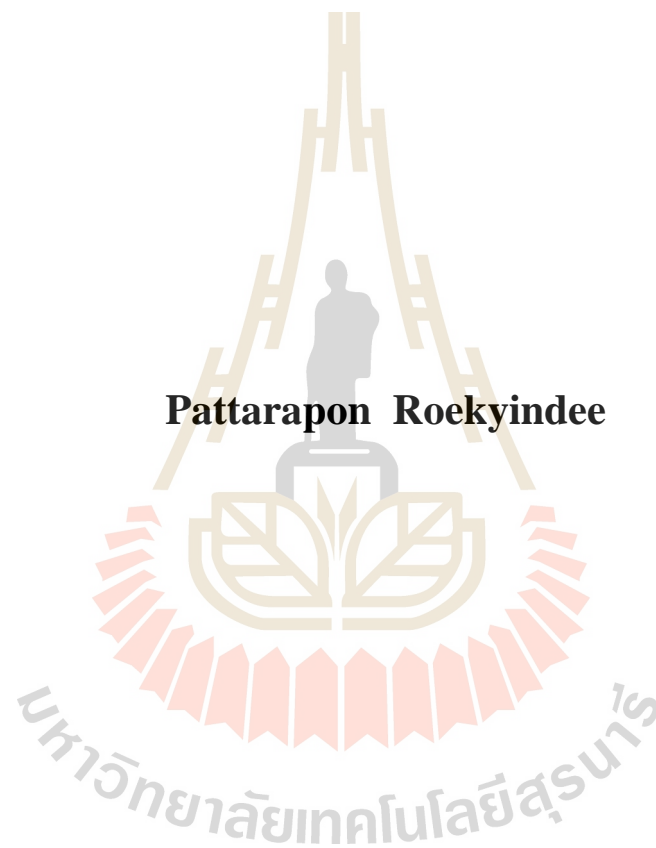


**EFFECTS OF ELASTIC MODULUS AND THICKNESS  
OF ROOF ON SUBSIDENCE CHARACTERISTICS**



**A Thesis Submitted in Partial Fulfillment of the Requirements for the  
Degree of Master of Engineering in Civil, Transportation  
and Geo-resources Engineering  
Suranaree University of Technology  
Academic Year 2019**

ผลกระทบของโมดูลสียืดหยุ่นและความหนาของหลังคา  
ต่อลักษณะการทรุดตัว




วิทยานิพนธ์นี้เป็นส่วนหนึ่งของการศึกษาตามหลักสูตรปริญญาวิศวกรรมศาสตรมหาบัณฑิต  
สาขาวิชาวิศวกรรมโยธา ขนส่ง และทรัพยากรธรณี  
มหาวิทยาลัยเทคโนโลยีสุรนารี  
ปีการศึกษา 2562

**EFFECTS OF ELASTIC MODULUS AND THICKNESS OF ROOF  
ON SUBSIDENCE CHARACTERISTICS**

Suranaree University of Technology has approved this thesis submitted in partial fulfillment of the requirements for a Master's Degree.


Thesis Examining Committee

  
\_\_\_\_\_  
(Assoc. Prof. Dr. Pornkasem Jongpradist)

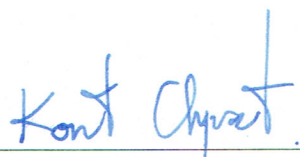
Chairperson

  
\_\_\_\_\_  
(Asst. Prof. Dr. Decho Phueakphum)


Member (Thesis Advisor)

  
\_\_\_\_\_  
(Asst. Prof. Dr. Akkhapun Wannakomol)

Member

  
\_\_\_\_\_  
(Assoc. Prof. Ft. Lt. Dr. Kontorn Chamniprasart)

Vice Rector for Academic Affairs and  
Internationalization

  
\_\_\_\_\_  
(Assoc. Prof. Dr. Pornsiri Jongkol)

Dean of Institute of Engineering

ภัทรภร ฤกษ์ยินดี : ผลกระทบของโมดูลัสยืดหยุ่นและความหนาของหลังคาต่อลักษณะการทรุดตัว (EFFECTS OF ELASTIC MODULUS AND THICKNESS OF ROOF ON SUBSIDENCE CHARACTERISTICS) อาจารย์ที่ปรึกษา : ผู้ช่วยศาสตราจารย์ ดร. เดโช เพ็ชร์ภูมิ, 48 หน้า.

แบบจำลองเชิงตัวเลขและเชิงกายภาพได้ดำเนินการเพื่อศึกษาผลกระทบของคุณสมบัติเชิงกลที่แปรผันของชั้นหินปิดทับ ความหนาหลังคาของช่องเปิด และความลึกของช่องเปิดต่อการทรุดตัวของพื้นผิวภายใต้สถานะที่ต่ำกว่าจุดวิกฤติ การศึกษามุ่งเน้นพิจารณาค่ามุมการไหลและการทรุดตัวสูงสุด ผลการศึกษาระบุว่าอัตราส่วนระหว่างการทรุดตัวสูงสุดและความสูงของช่องเปิดจะลดลงตามการเพิ่มขึ้นของความหนาหลังคาของช่องเปิด การทรุดตัวสูงสุดจะมีค่าคงที่เมื่ออัตราส่วนระหว่างความหนาหลังคาและความกว้างของห้องมีค่าเท่ากับหรือมากกว่า 0.4 การเพิ่มขึ้นของความลึกของช่องเปิดและค่าสัมประสิทธิ์ความยืดหยุ่นหลังคาของช่องเปิดสามารถลดค่าการทรุดตัวสูงสุดและเพิ่มค่าความกว้างของร่องการทรุดตัวบนผิวดิน การจำลองด้วยระเบียบวิธีเชิงตัวเลขโดยใช้โปรแกรม Phase 2.8 มีความสอดคล้องเป็นอย่างดีกับผลที่ได้จากแบบจำลองเชิงกายภาพ การค้นพบนี้สามารถใช้เพื่อคาดคะเนการทรุดตัวสูงสุด มุมการไหล และความกว้างของร่องการทรุดตัวของผิวดินที่เกิดจากการขุดเจาะเหมืองใต้ดินได้



PATTARAPON ROEKYINDEE : EFFECTS OF ELASTIC MODULUS  
AND THICKNESS OF ROOF ON SUBSIDENCE CHARACTERISTICS.

THESIS ADVISOR : ASST. PROF. DECHO PHUEKPHUM, Ph.D., 48 PP.

SUB - CRITICAL CONDITION/TROUGH/ANGLE OF DRAW/MAXIMUM  
SUBSIDENCE

Numerical and physical scale-down model simulations are carried out to study the effect of mechanical properties of overburden, roof thickness and opening depth on surface subsidence due to underground opening under sub-critical conditions. The study is focused on angle of draw ( $\gamma$ ) and maximum subsidence ( $S_{\max}$ ). The results indicate that the maximum subsidence-to-opening height ratios ( $S_{\max}/H$ ) decrease with increasing roof thicknesses. The maximum subsidence reaches constant, where the roof thickness-to-room width ratios ( $t/W$ ) are 0.4 or greater. The increasing of opening depth and elastic modulus of roof thickness can reduce the maximum subsidence and increase the trough width. The results of numerical simulations using Phase 2.8 program agree well with those obtained from the physical models. This finding can be used to predict the subsidence components due to underground excavation.

School of Geotechnology

Academic year 2019

Student's Signature P. Roekyindee

Advisor's Signature D. Phuekphum

## ACKNOWLEDGEMENT

First, I would like to express the Institute of Research and Development, Suranaree University of Technology for funded to this research.

I would like to thank my honest appreciation to Asst. Prof. Dr. Decho Phueakphum for his valuable guidance. I appreciate his powerful support, suggestions, and encouragement during the research period. I also would like to thank Professor Dr. Kittitep Fuenkajorn, Dr. Thanittha Thongprapha and Assoc. Prof. Dr. Pornkasem Jongpradist for valuable suggestions, support and comment on my research works. Grateful thanks to all staff of Geomechanics Research Unit who helped and supported my work and made me feel at home.

Lastly, I would like to thank my beloved mother for their love, support and encouragement.

Pattarapon Roekyindee

มหาวิทยาลัยเทคโนโลยีสุรนารี

# TABLE OF CONTENTS

	<b>Page</b>
ABSTRACT (THAI) .....	I
ABSTRACT (ENGLISH) .....	II
ACKNOWLEDGEMENTS .....	III
TABLE OF CONTENTS .....	IV
LIST OF TABLES .....	VII
LIST OF FIGURES .....	VIII
SYMBOLS AND ABBREVIATIONS .....	XII
<b>CHAPTER</b>	
<b>I INTRODUCTION .....</b>	<b>1</b>
1.1 Background and rationale.....	1
1.2 Research objectives.....	2
1.3 Scopes and limitations.....	2
1.4 Research methodology.....	3
1.4.1 Literature review.....	4
1.4.2 Computer simulation.....	4
1.4.3 Physical model testing.....	4
1.4.4 Comparisons of computer and physical model.....	4
1.4.5 Discussions and conclusions.....	4
1.4.6 Thesis writing.....	4

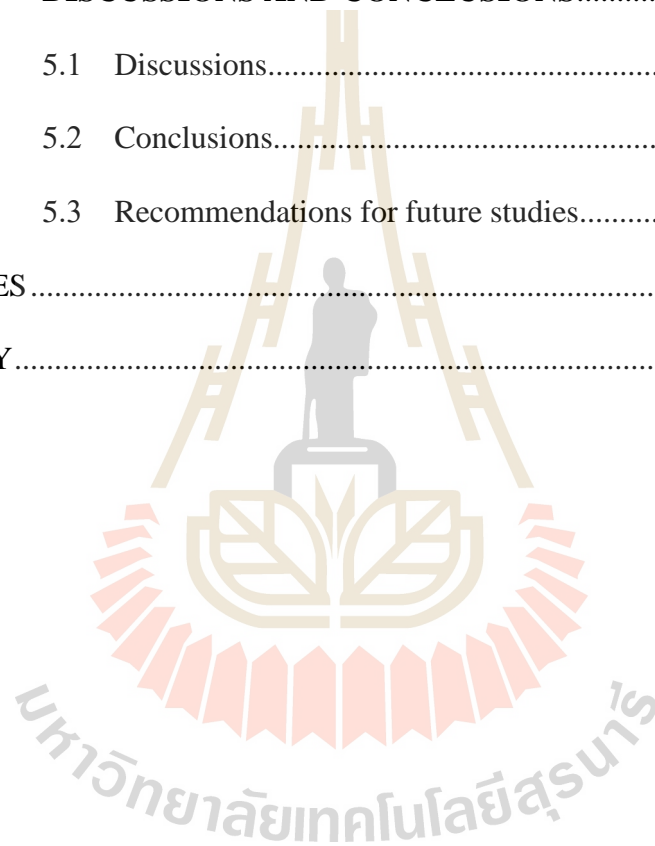
## TABLE OF CONTENTS (Continued)

	<b>Page</b>
1.5 Thesis contents.....	5
<b>II LITERATURE REVIEW .....</b>	<b>6</b>
2.1 Introduction.....	6
2.2 Theory and criterion.....	6
2.3 Numerical modeling.....	9
2.4 Physical modeling.....	11
2.5 Effect of underground opening geometries and overburden properties on surface subsidence.....	19
<b>III NUMERICAL SIMULATIONS.....</b>	<b>20</b>
3.1 Introduction.....	20
3.2 Finite difference analysis.....	20
3.2.1 Effect of roof thickness.....	21
3.2.2 Effect of opening depth.....	26
<b>IV PHYSICAL MODEL SIMULATIONS.....</b>	<b>30</b>
4.1 Introduction.....	30
4.2 Material property.....	30
4.3 Design and fabrication of test apparatus.....	33
4.4 Physical model simulation.....	35
4.5 Test results.....	38



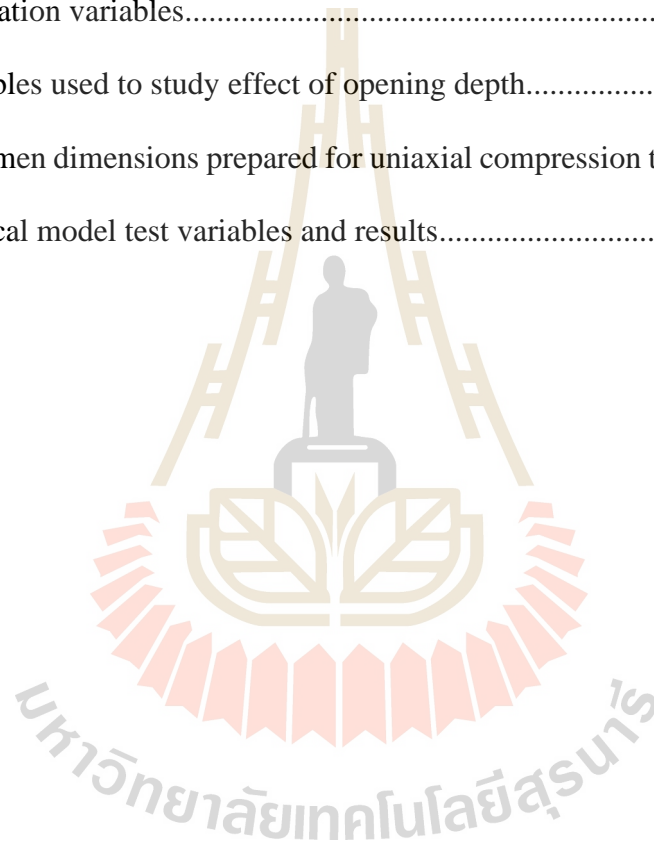
## TABLE OF CONTENTS (Continued)

	<b>Page</b>
4.6 Comparison of computer and physical model simulations.....	39
<b>V DISCUSSIONS AND CONCLUSIONS.....</b>	<b>42</b>
5.1 Discussions.....	42
5.2 Conclusions.....	43
5.3 Recommendations for future studies.....	43
REFERENCES .....	45
BIOGRAPHY .....	48



## LIST OF TABLES

Table	Page
3.1	Elasticity and density of Maha Sarakham formation.....22
3.2	Simulation variables.....24
3.3	Variables used to study effect of opening depth.....27
4.1	Specimen dimensions prepared for uniaxial compression testing.....32
4.2	Physical model test variables and results.....39



## LIST OF FIGURES

<b>Figure</b>		<b>Page</b>
1.1	Research methodology.....	3
2.1	Subsidence component.....	7
2.2	Schematic of ground movements caused by subsidence.....	8
2.3	Variables used by Aracheeploha et al.....	10
2.4	Basic subsidence mesh and model dimensions.....	11
2.5	(a) Trap door apparatus used for physical model testing (b) Mine opening is simulated by plastic blocks .....	12
2.6	Trap door apparatus used for physical model .....	13
2.7	$V_s/V_o$ as a function of opening depth ratio $Z/W$ and $H/W$ .....	13
2.8	Schematic diagram of the model box .....	14
2.9	Experimental setup .....	15
2.10	Graph suggested by NCB .....	16
2.11	A physical models for prediction of subsidence .....	17
2.12	Classical trap door problem .....	18
3.1	Boundary conditions and variable parameters used in numerical model simulations .....	21
3.2	Location of overburden above salt opening in the Maha Sarakham Formation (a) and stratigraphic units of borehole (b).....	22
3.3	Boundary conditions of individual (a) and averaged (b) overburden layers .....	23

## LIST OF FIGURES (Continued)

Figure	Page
3.4 Normalized maximum subsidence as a function of normalized roof thickness .....	25
3.5 Boundary conditions for series III simulation.....	26
3.6 Normalized subsidence vs normalize opening depth .....	28
3.7 Normalized limit trough wide vs of normalize opening depth .....	29
4.1 Synthetic gel mixed with paraffin under 60 oC planed in oven.....	30
4.2 Gel specimens prepared for uniaxial test .....	31
4.3 Gel specimen placed in a universal testing machine (UTM) .....	32
4.4 Stress-strain curves obtained from gel specimens with paraffin contents 30% by weight.....	34
4.5 Apparatus used for physical model testing .....	35
4.6 Variable used in simulations .....	36
4.7 (a) Synthetic gel (b) Synthetic gel melted into viscous fluid Under temperature of 60 °C.....	37
4.8 Filling synthetic gel into material container with pre-defined thickness .....	38
4.9 Maximum subsidence ( $S_{max}$ ) as a function of opening roof-to-opening width ratios ( $t/W$ ) .....	40

## LIST OF FIGURES (Continued)

<b>Figure</b>		<b>Page</b>
4.10	Trough wide (B) as a function of opening roof-to-opening width ratios (t/W) .....	40
4.11	Comparisons of subsidence profiles measured from physical and predicted by numerical model under various opening roof .....	41



## SYMBOLS AND ABBREVIATIONS

$B$	=	Limit trough wide
$D$	=	Depth of opening
$E$	=	Elastic modulus of overburden
$E_{ave}$	=	Average modulus
$E_{ore}$	=	Elastic modulus of ore
$H$	=	Height of opening
$S_{max}$	=	Maximum subsidence
$t$	=	Thickness roof of opening
$W$	=	Width of opening
$\gamma$	=	Angle of draw
$\nu$	=	Poisson's ratio
$\rho$	=	Density
$\rho_{ave}$	=	Average density
$\rho_{ore}$	=	Density of ore
$\sigma_c$	=	Uniaxial compressive strength
$\sigma_t$	=	Tensile strength

# CHAPERT I

## INTRODUCTION

### 1.1 Background and rationale

Surface subsidence due to underground mining can affect surface structures within the mine area (Asadi et al., 2005). Several parameters control the magnitude and extent of depression area that occur due to underground mining (Henry, 1956; King and Whetton, 1957; Brauner, 1973). The observed data and theoretical studies show that the subsidence for underground mining is related to following factors: mining depth, mining thickness, degree of extraction, methods of working, near-surface geology, physical and mechanical properties of overburden and ore seam (Yao et al., 1991; Liu et al., 2013). Overburden strata and ore seam properties is one of the important factors that control the surface subsidence characteristics (Yao et al., 1991). Most researchers tried to correlate the subsidence characteristic (maximum subsidence and angle of draw) with overburden strata and ore seam properties for underground mining under sub-critical, critical, and super-critical conditions using physical and numerical methods (Thongprapha et al., 2015; Sartkeaw et al., 2016; Saoanunt et al., 2018). These are research considered the overburden strata to be homogenous and only one type of overburden rock. Multi-layers of overburden rock strata and the difference in their mechanical properties are not emphasizing as the key parameter for the study. Even though numerous studies have been carried out to analyze and simulate the surface subsidence under various configurations of underground opening, rare attempt has been

made to assess the effects of overburden properties, in particular, modulus of deformation (for sub-critical condition).

## 1.2 Research objectives

The goal of this study is to determine the relationships between deformation modulus ( $E$ ) of the overburden with the subsidence components, particularly trough width and subsidence magnitude ( $S_{\max}$ ) under sub-critical condition. Phase 2.8 to simulate the surface subsidence as effected by mechanical properties of overburden, roof thickness and opening depth. The Synthetic gel and paraffin wax are used to represent the overburden. The result from the computer simulation are compared with of the physical model to assess the accuracy of the test results.

## 1.3 Scopes and limitations

- 1) Finite difference method (Phase 2.8) in used to simulate the subsidence characteristics as affect by mechanical properties of overburden, roof thickness and opening depth on surface subsidence.
- 2) The roof thickness in numerical simulation is varied from 0 to 20 m. The elastic modulus of roof thickness of overburden is simulated from 0.1, 0.5, 1.5, 5 to 10 GPa, and opening depth is selected from 80, 180, 280, 380 to 480 m.
- 3) The experiments are interested on the maximum subsidence, angle of draw and trough width which occurring due to roof thickness.
- 4) Synthetic gel and paraffin wax are prepared to simulate the elastic overburden.
- 5) Subsidence of the model is induced by real gravitational force.



6) Physical model results are compared with the analytical methods given by Singh (1992) and with numerical simulations (using Phase 2.8 software).

7) The main focus is on the sub-critical subsidence induced by manmade underground openings (e.g. mines, tunnels and caverns).

#### 1.4 Research methodology

The research methodology shown in Figure 1.1 includes 6 steps; literature review, computer simulation (Phase 2.8), physical model testing, comparisons, discussions and conclusions, and thesis writing.

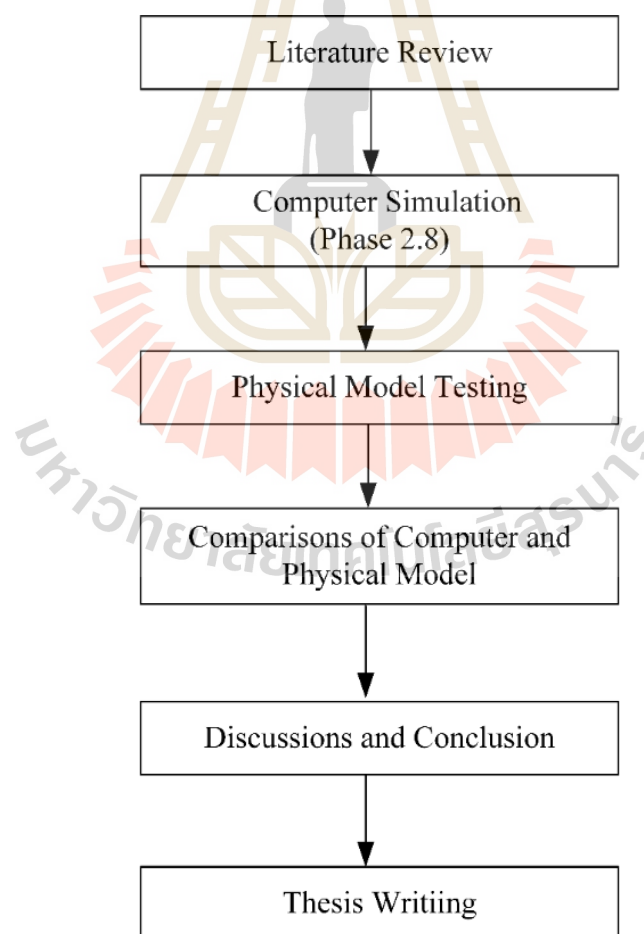


**Figure 1.1** Research methodology

#### **1.4.1 Literature review**

Literature review is carried out to improve an understanding of sub-critical surface and case studies. The information are from journals, and conference papers.

#### **1.4.2 Computer simulation**

The computer programs are used to calculate the characteristics of the subsidence model by considering the effects of underground opening geometries. Phase 2.8 software are used for the calculation. The results from the calculation are compared with the model testing.

#### **1.4.3 Physical model testing**

The scale-down is used to simulate subsidence characteristics. The laboratory testing is measured the maximum magnitude of subsidence at sub-critical point ( $S_{max}$ ), angle of draw, and hence allowing studying the effect of overburden properties and underground opening geometries on ground surface.

#### **1.4.4 Comparisons of computer and physical model**

The finite difference analyses (Phase 2.8) are used to calculated the characteristics of the subsidence. The results obtained from computer simulation results (Phase 2.8) are compared with the physical model testing.

#### **1.4.5 Discussions and conclusions**

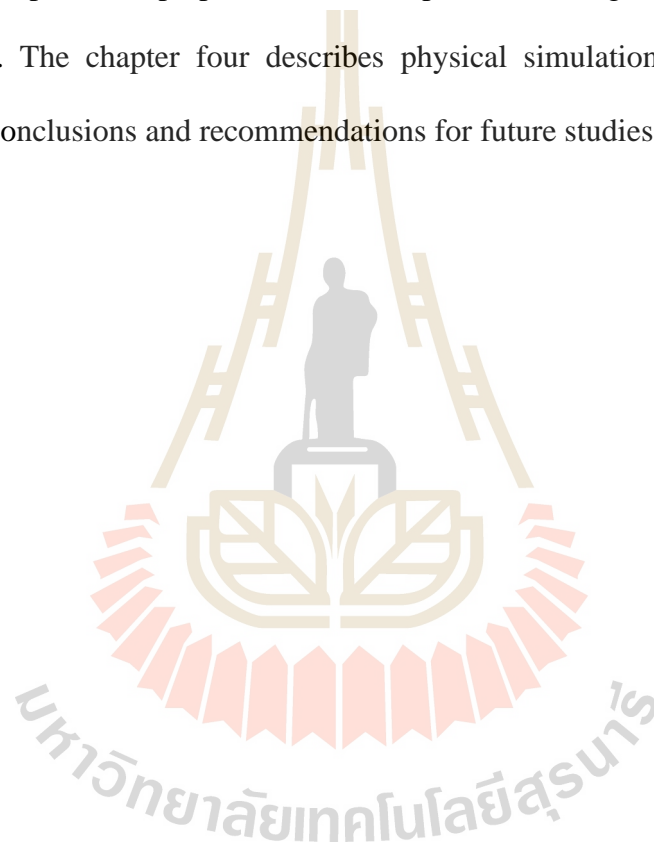
Discussions are made on the test results.

#### **1.4.6 Thesis writing**

All research activities, methods and results are documented and compiled in the thesis.

## 1.5 Thesis contents

This research thesis is divided into five chapters. The first chapter includes background and rationale, research objectives, scope and limitations and research methodology. The second chapter shows results of the literature review to improve an understanding of surface subsidence knowledge and case studies in Thailand and abroad. The chapter three proposes subsidence prediction using finite difference method by Phase 2.8. The chapter four describes physical simulation. Chapter five gives discussions, conclusions and recommendations for future studies.



# CHAPERT II

## LITERATURE REVIEW

### 2.1 Introduction

This chapter presents the results of literature review which include the effects of underground opening geometries and overburden properties on surface subsidence, surface subsidence prediction, physical modeling, empirical subsidence calculation and numerical simulations. The review results are summarized below.

### 2.2 Theory and criterion

Singh (1992) states that subsidence is a consequence of underground mining – it may be extended over localized or large areas and smaller, it may be immediate or delayed for many years. With the increased concern for the environment and expansion of urbanization, it cannot longer possible to ignore its aftermath. The principle goals of subsidence study are 1) Prediction of ground displacement 2) Determining the effects of renewable resource, and 3) Reduction damage due to surface subsidence. When the area of surface collapse into the mine void is relatively small, the subsidence is termed a pit or sinkhole, generally, these are associated with shallow room and pillar mining. This implies that the diameter of the area of influence is given by  $2D \tan\gamma$ , where  $D$  is the depth of the seam below the surface and  $\gamma$ , where  $D$  is the depth of the seam under the surface, and  $\gamma$  is the limit angle. If a super-critical width is excavated, a flat-bottomed depression will be produced. Subsidence consists of five principle

components, including vertical curvature, vertical strain, horizontal displacement, vertical displacement and slope (Figure 2.2).

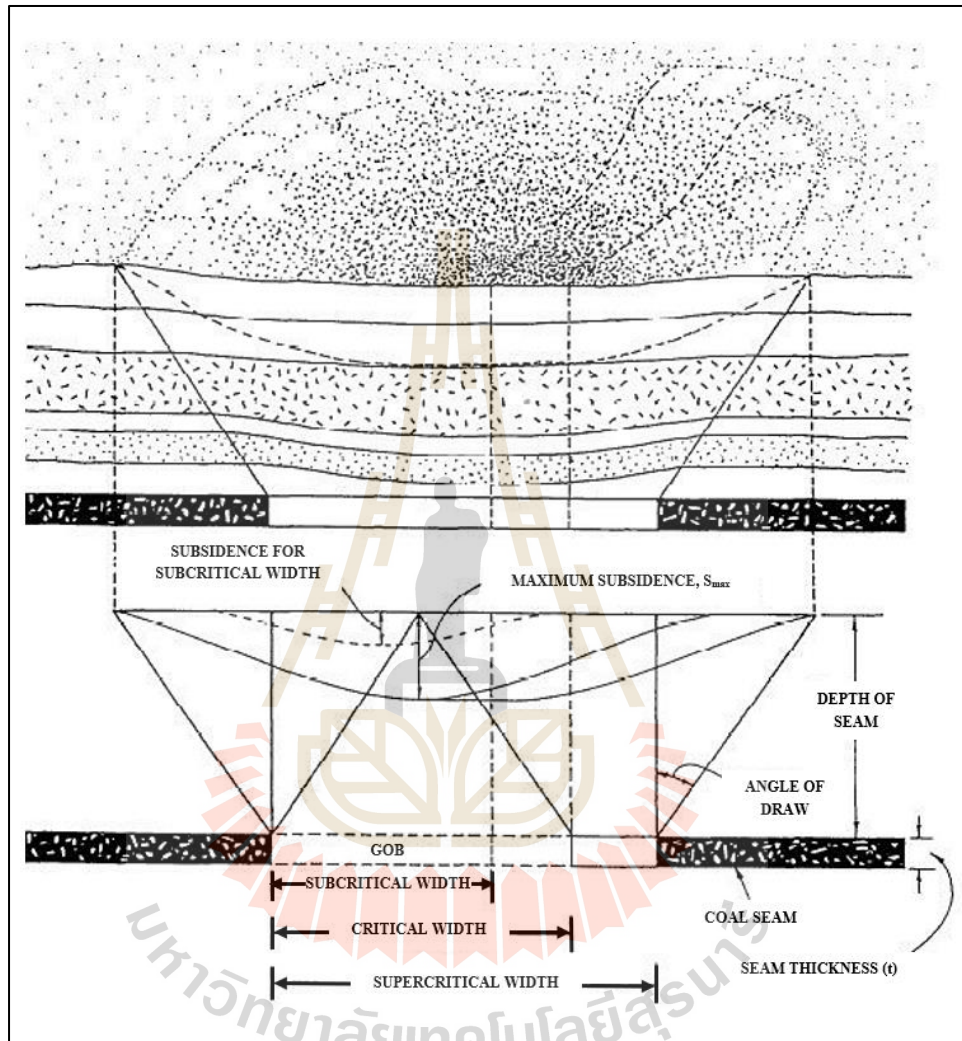


**Figure 2.1** Subsidence component (Singh, 1992)

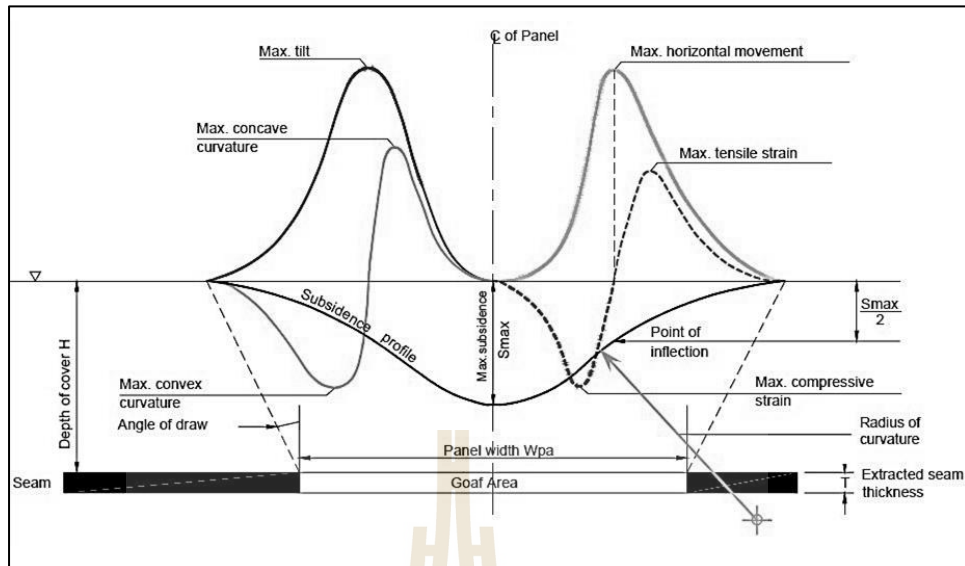


**Figure 2.2** Schematic of ground movements caused by subsidence

Calculation by profile function;

Vertical displacement:

$$S(x) = 0.5S_{\max} \left[ 1 - \tanh\left(\frac{cx}{B}\right) \right] \quad (2.1)$$

Slope (or tilt):

$$G(x) = S'(x) = -0.5S_{\max} \left(\frac{c}{B}\right) \operatorname{sech}^2\left(\frac{cx}{B}\right) \quad (2.2)$$

Vertical curvature:

$$\rho(x) = S''(x) = S_{\max} \left(\frac{c^2}{B^2}\right) \left[ \operatorname{sech}^2\left(\frac{cx}{B}\right) \tanh\left(\frac{cx}{B}\right) \right] \quad (2.3)$$

Horizontal displacement (lateral movement):

$$u(x) = -0.5 S_{\max} \left(\frac{bc}{B}\right) \operatorname{sech}^2\left(\frac{cx}{B}\right) \quad (2.4)$$

Horizontal strain:

$$\varepsilon(x) = S_{\max} \left(\frac{bc^2}{B^2}\right) \left[\operatorname{sech}^2\left(\frac{cx}{B}\right) \tanh\left(\frac{cx}{B}\right)\right] \quad (2.5)$$

Where

- $S_{\max}$  = Maximum surface subsidence
- $D$  = Opening or cavern depth
- $B$  = Cavern maximum radius
- $\gamma$  = Angle of draw
- $c$  = Constant value
- $b$  = Constant value
- $x$  = Horizontal distance

### 2.3 Numerical modeling

Aracheeploha et al. (2009) develop an analytical method to evaluate the location, size and depth of the caverns crated at the interface between overlying and salt formations. Hyperbolic function is used in the survey data statistical analysis to determine the maximum subsidence, cavern location, slope or tilt and curvature under critical and sub-critical conditions. Numerical simulation is evolution to execute the produce a set and regression of surface subsidence components and a representative profile of the surface subsidence. The empirical equations correlate subsidence components with the overburden properties and cavern configurations. For the super-critical condition, a

discrete element method (DEM) using UDEC software is used to simulate the uncertainties of the sinkhole development and ground displacement resulting from the overburden post-failure deformation and joint movement complexity. The correlations of the subsidence components with the overburden properties and cavern geometries are applicable to a range of actual conditions especially assigned here (e.g., half oval-shaped cavern created in flat ground surface, saturated condition, overburden-salt interface, and horizontal rock units).

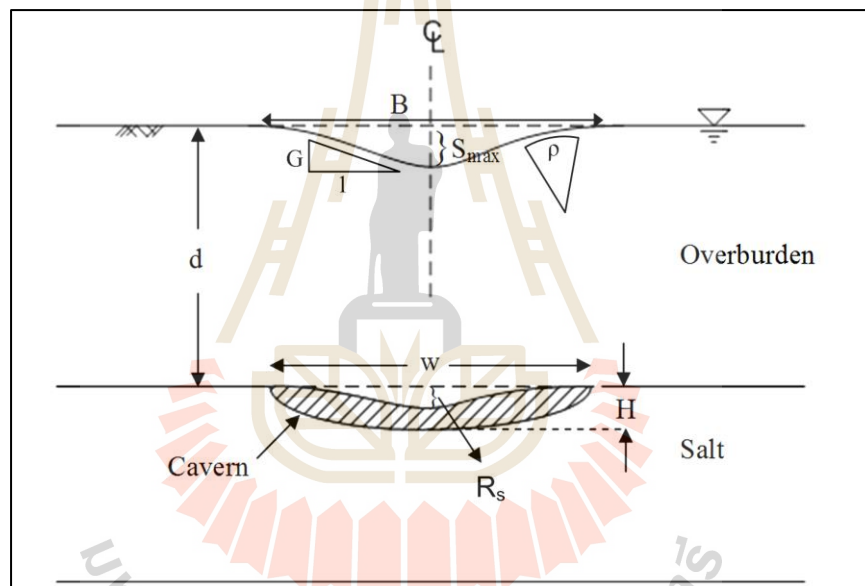


**Figure 2.3** Variables used by Aracheeploha et al. (2009)

Ren and Li (2008) study the extent of mining subsidence. The affected area is defined by the angle of draw, which is predominantly controlled by the mining configurations and overburden strata. The strength, stiffness and failure of the overburden play an important role in the characteristics of maximum subsidence. When overburden rocks are broken up taking place in the roof and sufficiently strong, the angle of draw would tend to be greater in roof rocks with greater than stiffness. However,



if the roof failure, weak roof strata would result in greater angle of draw and stronger strata would produce lower angle of draw at the surface. Normally the maximum subsidence over a weak overburden is greater than over a strong overburden. Computer model has demonstrated that the effect of seam inclination is such that it reduces the angle of draw at the rise-side of the panel and increases the angle of draw.

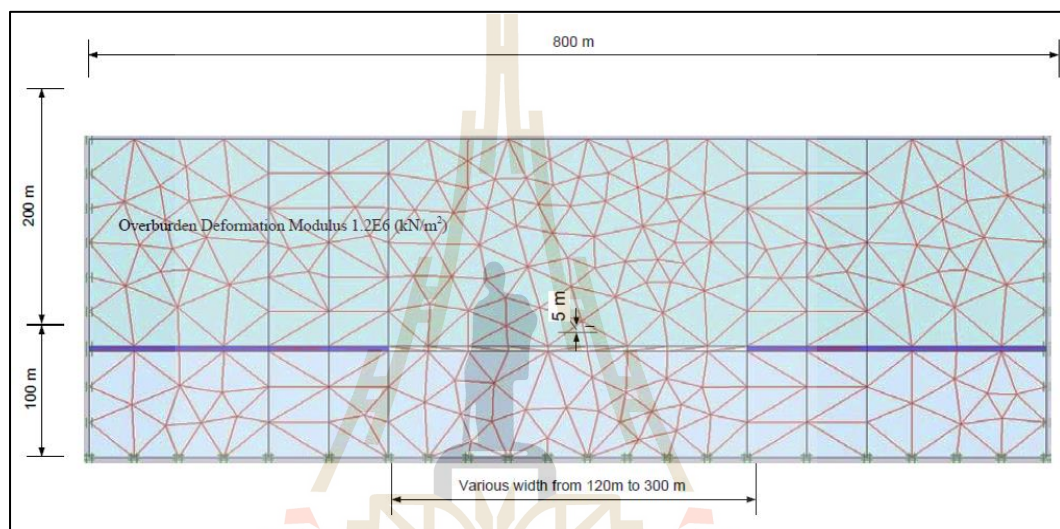


**Figure 2.4** Basic subsidence mesh and model dimensions (Ren and Li, 2008)

## 2.4 Physical modeling

Sartkaew and Fuenkajorn (2016) perform physical models to verify the accuracy and representativeness of the hyperbolic, trigonometric profile functions and exponential that have been commonly used to define the surface subsidence under sub-critical conditions induced by salt and potash mining. A trap door apparatus is used to model the surface subsidence and to evaluate the effects of the depth and opening geometry (Figure 2.5). The results present the opening width increasing with increasing angle of draw. Angle of draw more sensitive to  $W$  than  $Z$ .

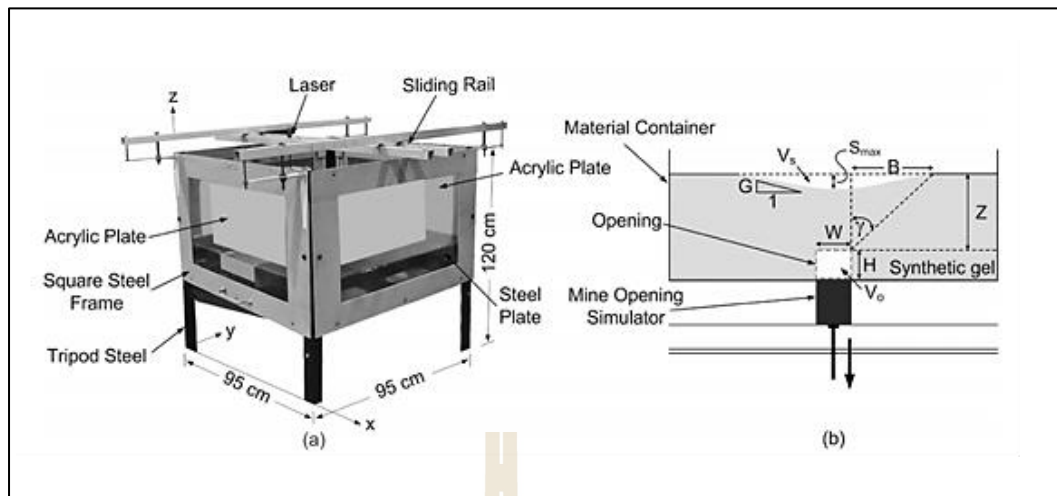


**Figure 2.5** (a) Trap door apparatus used for physical model testing

(b) Mine opening is simulated by plastic blocks

(Sartkaew and Fuenkajorn, 2016)

Thongprapha et al. (2015) use physical models to study the effects of underground opening on subsidence under super-critical conditions. Figure 2.6 shows variables apparatus used in physical model. Clean gravel is used to represent the overburden. The results indicate the volume of trough, angle of draw and maximum subsidence are controlled by the depth, width and length of the underground mining. The tends to approach a limit when  $L/W$  equals 3 and angle of draw and maximum subsidence increase with increasing  $L/W$  ratio. For the same  $H/W$  ratio and  $L/W$  ratio, increasing the  $Z/W$  ratio decreases the maximum subsidence and angle of draw. Figure 2.7 shows the volume of subsidence trough observed from the opening volume is always greater than the physical model.

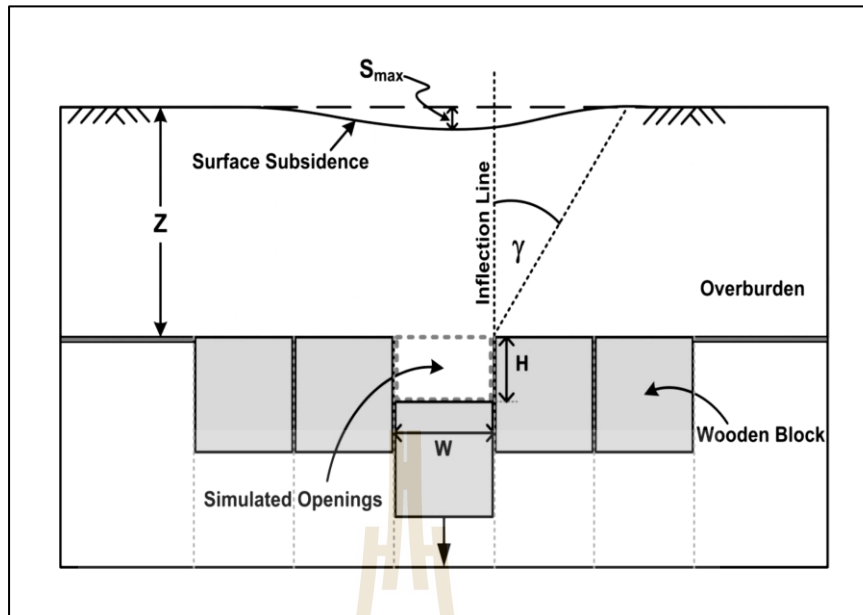


**Figure 2.6** Trap door apparatus used for physical model (Thonggrapha et al., 2015)

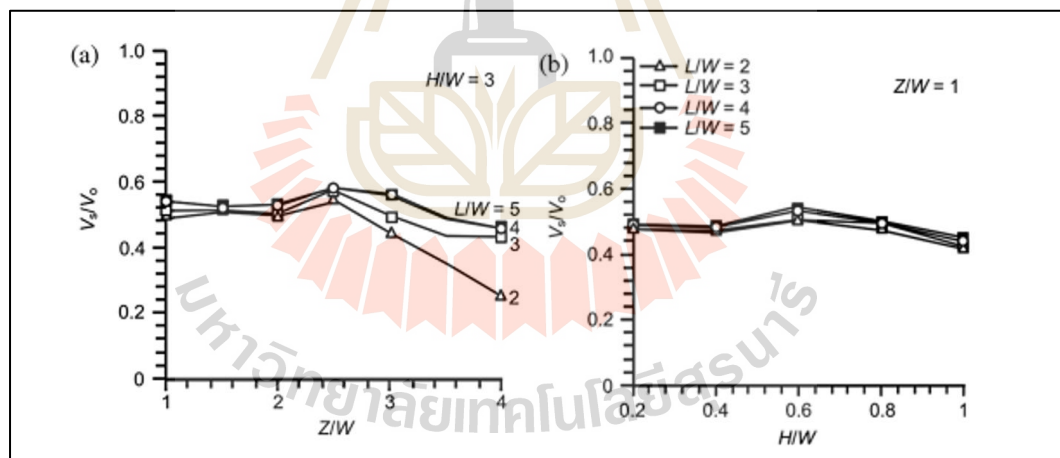


**Figure 2.7**  $V_s/V_0$  as a function of opening depth ratio  $Z/W$  and  $H/W$

(Thonggrapha et al., 2015)

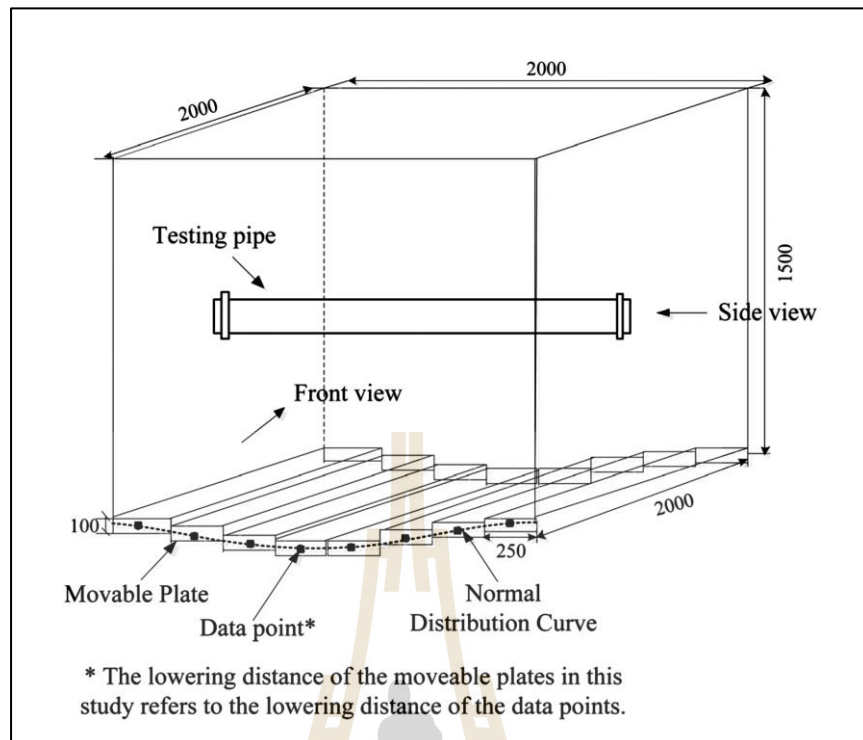


**Figure 2.8** Schematic diagram of the model box (Wang et al., 2015)

Wang et al. (2015) study the effects of the existence of the service pipelines on the ground displacement induced by tunneling. The test results indicate that HDPE pipes resulted in a wider but shallower trough width than in the greenfield (without pipe) case. The width of the trough width at a given depth increased with increasing buried depth of the pipe, whereas it decreased with increasing pipe diameter.

Saoanunt and Fuenkajorn (2015) study the effects of the mining sequences, excavation rates and overburden slope under super-critical condition. They found that the angle of draw and  $S_{\max}/H$  ratio decrease with increasing  $Z/H$  ratio when the opening height ( $H$ ) is maintained constant at 50 mm and the opening depth ( $Z$ ) varies from 50 mm to 200 mm. Consecutive mining sequence from center of panel gives the lowest angle of draw and highest subsidence while excavation from the edge to center of panel causing

the highest angle of draw and lowest subsidence. Under various overburden slopes, the angle of draw on up-slope and down-slope increases with increasing slope angle. The  $S_{\max}/H$  ratio decreases with increasing  $Z/H$  ratio and slope angle.

Tunsakul et al. (2013) study the failure behavior of rock mass around gas storage cavern with physical model test. They designed the physical character of model test is a silo, 0.1 meter in diameter, 0.2 meter in height and the location of the cavern center is 0.5 meter under the ground surface. The rocks are simulated from mixture of plaster, sand and water. The test arrangement is shown in Figure 2.9. They conclude that the lateral earth pressure has strong influence on the position of the initial points as obtained by numerical analyses.

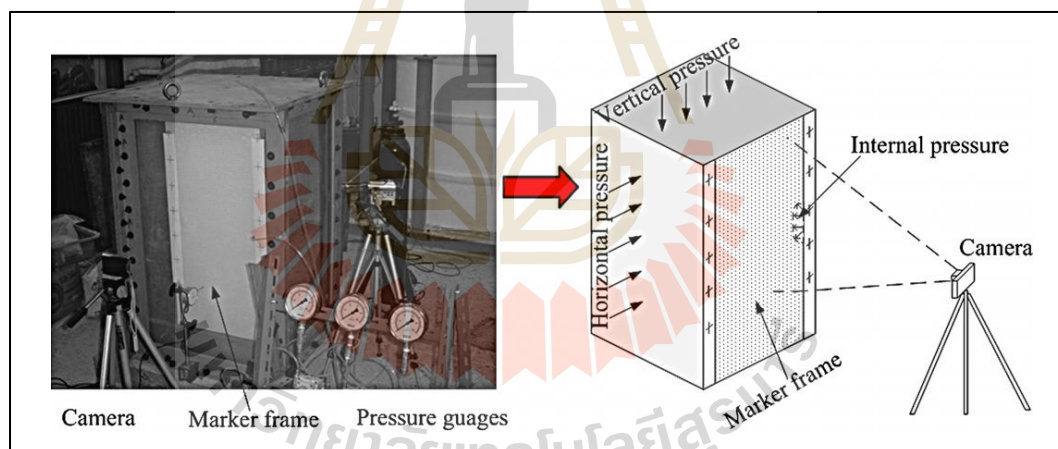


**Figure 2.9** Experimental setup (Tunsakul et al., 2013)

Caudron et al. (2006) find that physical models allow to present a case study and to define it absolutely with limited set of parameters. They study interaction of soil in a sinkhole phenomenon using analog 2D physical model and numerical simulation. The material in simulations is used the bi-dimensional Schneebeli material.

Asadi et al. (2005) propose a new profile function. It is from the sum of two negative exponential functions that have been adjusted to three survey lines in a case study in the Negin coalmine east of Iran. Because of the simplicity of the profile function, the use of the new model decreases the calculation time for predicting surface subsidence and enhances the precision of subsidence prediction. The results show good correlation between the measured and the predicted subsidence. In the empirical method, different graphs and tables are given for different conditions and geometrical shapes. It is possible to predict the amount of subsidence using these graphs and tables. The National Coal Board (NCB) has suggested one of the most well-known graphs for the prediction of subsidence. For example, a graph for the prediction of surface subsidence in horizontal stopes is given in Figure 2.10.

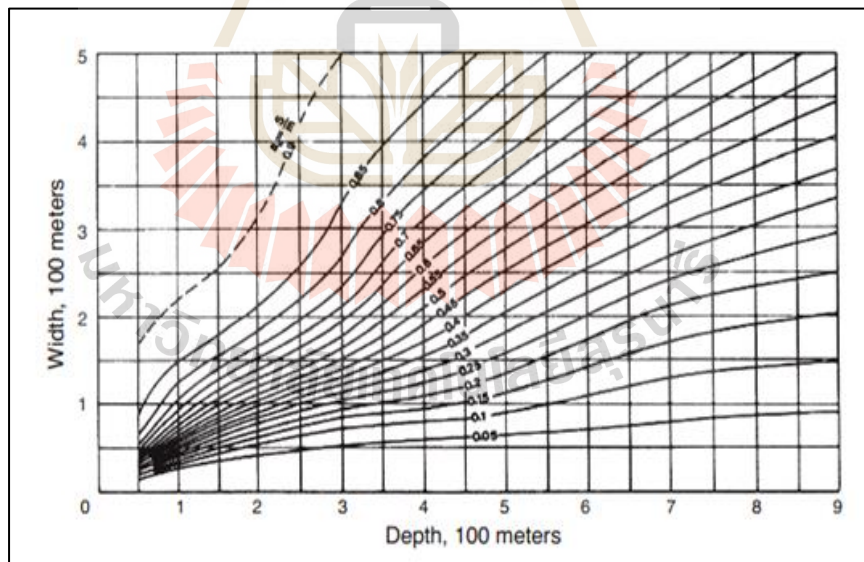


**Figure 2.10** Graph suggested by NCB (Asadi et al., 2005)

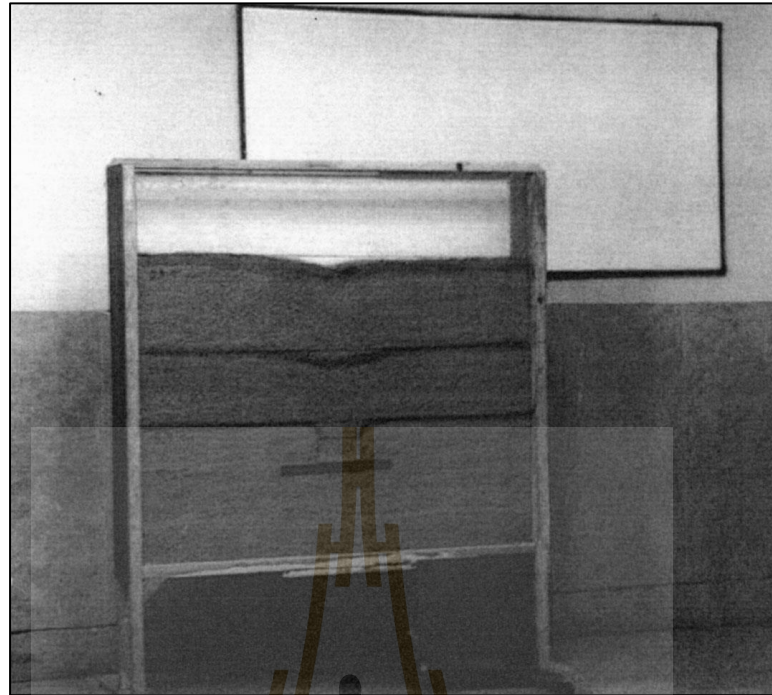


**Figure 2.11** A physical models for prediction of subsidence (Asadi et al., 2005)

Park et al. (2004) conclude that surface movement cause damage to the deterioration and failure of infrastructures, building, underground utility lines, dams, etc., resulting in environmental hazards and severe economic loss. In order to prevent or minimize subsidence damage, it is important to understand subsidence spectacle. It is difficult to predict or model subsidence evolution because of the complexity in physical simulation such as yield behavior and rock failure, time dependent behavior and dimensional variations.

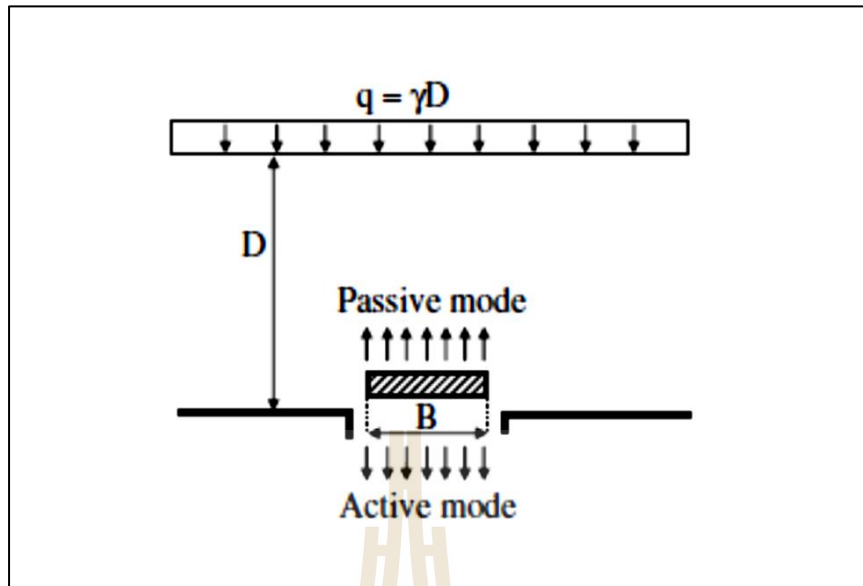


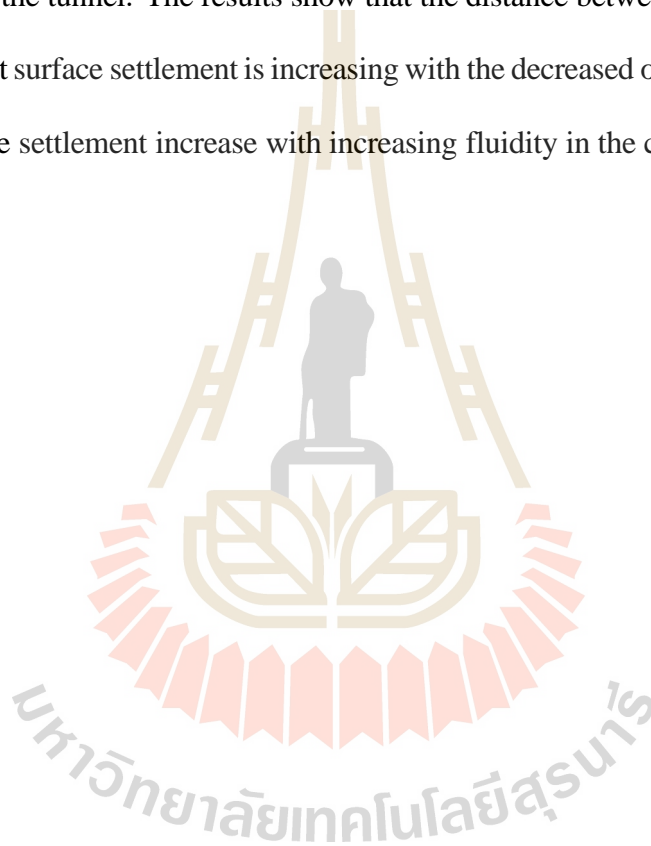
**Figure 2.12** Classical trap door problem (Terzaghi, 1936)

Terzaghi (1936) uses a simulation, characterized as the trap-door model to explain the arching theory based on the translation of a trap door away from it (active mode) or into the soil (passive mode). The active mode can be used to study the earth pressure on a tunnel lining or the silo problem. The passive mode can be used to estimate of the other buried structures and uplift force of anchors that can be idealized as anchors. The deforming arch of a opening can be investigated by a downward moving trap-door while the soil above the opening can be represented by a slightly cohesive soil or layer of granular. Based on this simple simulation, the development of the mean vertical pressure acting on the trap-door during its downward movement can be studied. The physical simulation allowed him to shows determine it fully and case study with a limited set of parameters.



## **2.5 Effect of underground opening geometries and overburden properties on surface subsidence**

Jiang and Yin (2014) investigated the effect of soil conditions on the ground deformation during longitudinal tunneling. Different cases of soil conditioning were modeled by reducing the inter-particle friction of soils in the specified zone around the cutter head of the tunnel. The results show that the distance between the final cutter face and the biggest surface settlement is increasing with the decreased of inter-particle friction and the surface settlement increase with increasing fluidity in the conditioning zone.



## CHAPTER III

### NUMERICAL SIMULATIONS

#### 3.1 Introduction

This chapter describes the results of finite difference analysis using Phase 2.8 (Rocscience Inc., 2012). The primary objective is to determine the effect of deformation modulus ( $E$ ) of overburden, opening depth and roof thickness on surface subsidence in terms of subsidence magnitude ( $S_{\max}$ ) and angle of draw ( $\gamma$ ).

#### 3.2 Finite difference analysis

Phase 2.8 is a two dimensions finite difference stress analysis program for designing and excavations of underground opening. It can be used for rock or soil applications. In this study, the computer model simulations are performed to study the surface subsidence trough under sub-critical condition correlating with the opening roof thickness, mechanical properties of the overburden and the opening depth.

Over 8,000 uniform mesh with three node triangle element types have been constructed to obtain accurate simulation results. The analyses are performed under plane strain condition. The distance from left and right boundaries to the center is 1010 m. The left and right edges are fixed in the x-axis and the bottom boundary is fixed in the y-axis. The upper boundary can move freely in both directions. The floor of the opening is constant at 70 m. Figure 3.1 present the parameters used to the simulation. They include opening depth ( $D$ ), opening width ( $W$ ), opening height ( $H$ ), roof thick ( $t$ ), maximum subsidence ( $S_{\max}$ ), limit trough wide ( $B$ ) and angle of draw ( $\gamma$ ).

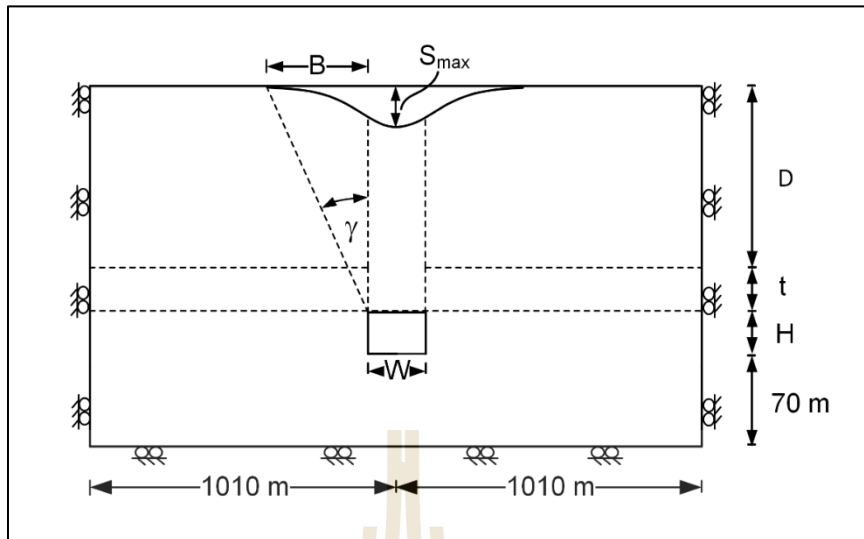


**Figure 3.1** Boundary conditions and variable parameters used in numerical model simulations.

### 3.2.1 Effect of roof thickness

The goal of this study is to determine influence of various roof thickness on surface subsidence. The overburden properties are obtained from typical borehole data drilled in the Maha Sarakham formation at Ban Khao, Muang district, Udon Thani, northeast of Thailand. Figure 3.2 shows the location and typical stratigraphic sections of the borehole. The physical and mechanical properties used in Phase 2.8 simulation are shown in Table 3.1. The elastic modulus of salt is 19.90 GPa and density of lower salt member is  $2,130 \text{ kg/m}^3$  (Crosby, 2007; Wetchasat, 2002).

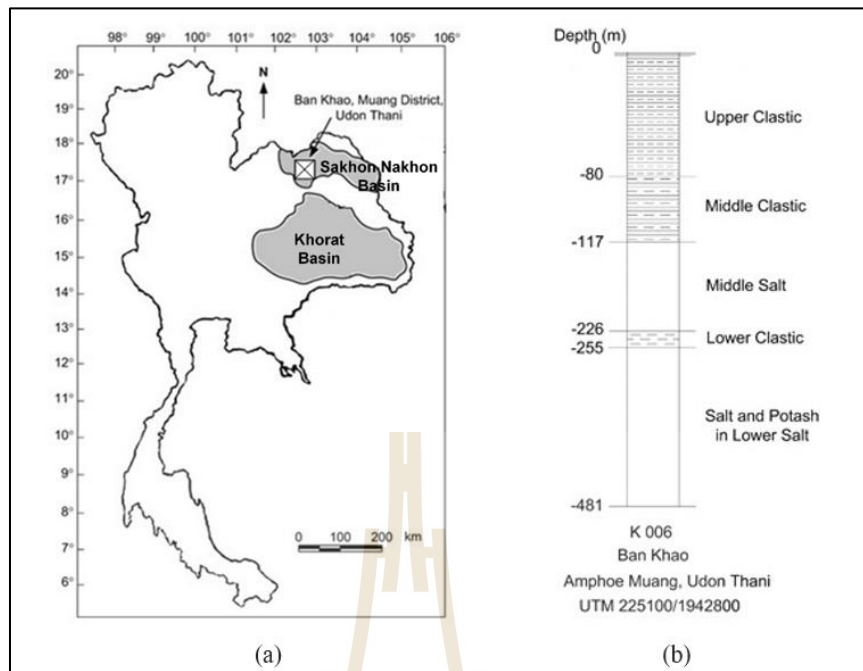


**Figure 3.2** Location of overburden above salt opening in the Maha Sarakham formation (a) and stratigraphic units of borehole (b) (Crosby, 2007; Wetchasat, 2002)

**Table 3.1** Elasticity and density of Maha Sarakham formation

Rock unit	Thickness ( $t_i$ )	Density ( $\rho_i$ )	Elastic modulus ( $E_i$ )	Poisson's Ratio ( $\nu$ )	Compressive strength ( $\sigma_c$ )	Tension ( $\sigma_t$ )
	(m)	( $\text{kg/m}^3$ )	(GPa)	-	(MPa)	(MPa)
Upper Clastic	80	2,490	3.80	0.23	0.83	0.47
Middle Clastic	37	2,160	0.47	0.21	1.52	1.00
Middle Salt	109	2,490	2.42	0.24	18.23	0.83
Lower Clastic	29	2,160	3.24	0.26	6.21	0.81
Lower salt	226	2,130	19.90	0.24	19.15	1.88

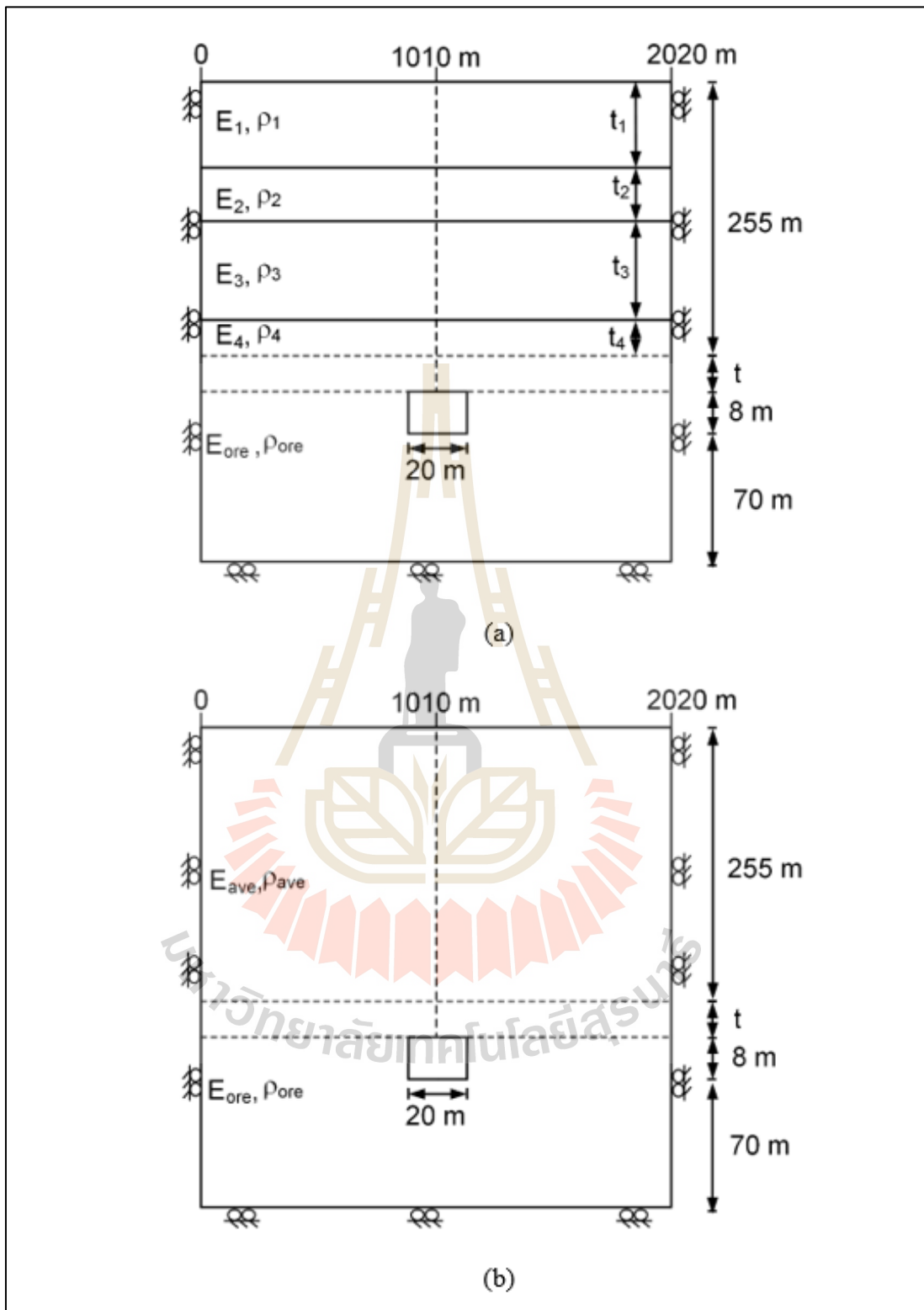


**Figure 3.3** Boundary conditions of individual (a) and averaged (b) overburden layers

**Table 3.2** Simulation variables.

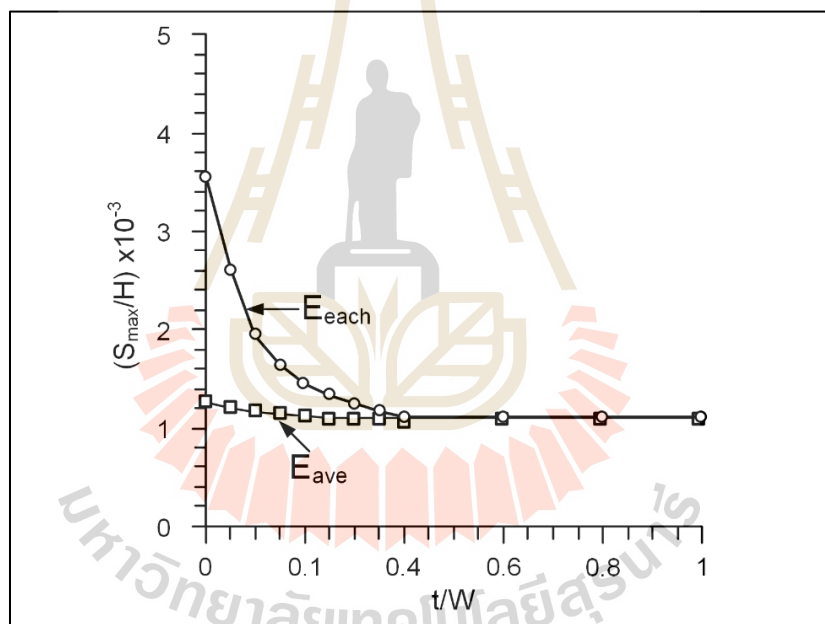
Parameters		Individual overburden layer			Averaged overburden layer		
Roof thickness-to-opening width ratio (t/W)	Roof Thickness t (m)	S <sub>max</sub> (mm)	B (m)	γ (degree)	S <sub>max</sub> (mm)	B (m)	γ (degree)
0.00	0	3.58	664.34	67.51	1.25	700.74	68.57
0.05	1	2.61	631.99	66.48	1.20	662.32	67.45
0.10	2	1.88	617.84	66.01	1.18	642.1	66.82
0.15	3	1.62	605.71	65.58	1.14	629.97	66.42
0.20	4	1.43	593.57	65.14	1.11	621.88	66.14
0.25	5	1.27	589.53	64.99	1.10	613.79	65.87
0.30	6	1.14	585.49	64.84	1.08	609.75	65.72
0.35	7	1.08	585.49	64.84	1.03	605.71	65.58
0.40	8	1.05	575.38	64.45	1.03	605.71	65.58
0.60	12	1.05	571.33	64.30	1.03	597.62	65.29
0.80	16	1.05	571.33	64.30	1.03	597.62	65.29
1.00	20	1.05	571.33	64.30	1.03	597.62	65.29

To study the effect of complex and non-uniformity of rock strata on the surface subsidence, the elastic modulus and the density of the overburden above ore are considered under two conditions (Figure 3.3) 1) the overburden with different mechanical properties of each layer and 2) the overburden with average properties from all layers. The average modulus ( $E_{ave}$ ) and density ( $\rho_{ave}$ ) of overburden above the lower salt layer can be calculated as follows:

$$E_{ave} = \frac{\sum_{i=1}^n E_i t_i}{\sum_{i=1}^n t_i} \quad (3.1)$$

$$\rho_{ave} = \frac{\sum_{i=1}^n \rho_i t_i}{\sum_{i=1}^n t_i} \quad (3.2)$$

where  $i$  is number of rock unit. From the above equation, the  $E_{ave}$  and  $\rho_{ave}$  are calculated as 2.66 GPa and 2,405 kg/m<sup>3</sup>, respectively.



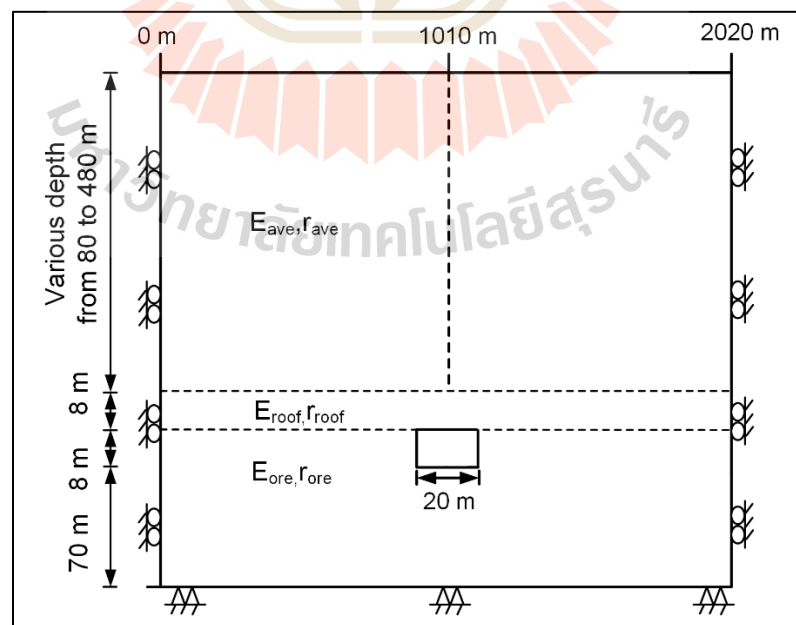
**Figure 3.4** Normalized maximum subsidence as a function of normalized roof thickness

Figure 3.4 shows the relationship between  $S_{max}/H$  ratio and  $t/W$  ratio. The results indicate that  $S_{max}/H$  ratios decrease with increasing roof thickness. The maximum subsidence reaches constant, where the roof thickness-to-opening width ratios are greater than 0.4. The roof thickness at  $t/W$  ratio equal 0.4 is where the

maximum subsidence of  $E_{each}$  and  $E_{ave}$  are equal. Therefore, when  $t/W$  ratios are greater than 4.0, the subsidence value of  $E_{each}$  and  $E_{ave}$  will be equal. This suggests that the average properties of overburden can be used accurately when  $t/W$  ratios are 0.4 or greater. This makes the subsequent simulation much more simples.

### 3.2.2 Effect of opening depth

The objective of this study is to study the effect of opening depth on subsidence trough. All cases are simulated under constant opening width of 20 m, and with 8 m opening height. The elastic modulus of ore ( $E_{ore}$ ) of overburden is 1 GPa, the elastic modulus of roof thickness ( $E_{roof}$ ) of overburden are varied from 0.1, 0.5, 1.5, 5 and 10 GPa. The average elastic modulus ( $E_{ave}$ ) of overburden is 0.1 GPa. In this section the average elastic modulus of averaged overburden layer is selected to simulate the overburden subsidence. The depths of opening ( $D$ ) are varied from 80, 180, 280, 380 to 480 m (Figure 3.5). The variables used in the simulation are shown in Table 3.3.



**Figure 3.5** Boundary conditions for series III simulation



**Table 3.3** Variables used to study effect of opening depth.

Parameters		Results		
Depth, D (m)	Elastic modulus of roof, $E_{\text{roof}}$ (GPa)	$S_{\text{max}}$ (mm)	B (m)	$\gamma$ (degrees)
80	0.1	28.39	120.29	56.37
	0.5	10.41	142.73	60.73
	1.5	7.32	145.23	61.15
	5	5.97	147.13	61.47
	10	5.29	150.00	61.93
180	0.1	9.13	270.66	56.37
	0.5	6.37	283.94	57.63
	1.5	5.01	283.94	57.63
	5	4.99	283.94	57.63
	10	4.30	288.59	58.05
280	0.1	4.64	479.04	59.69
	0.5	4.09	475.54	59.51
	1.5	3.94	475.54	59.51
	5	3.48	475.54	59.51
	10	3.48	479.04	59.69
380	0.1	4.45	618.21	58.42
	0.5	3.87	604.19	57.83
	1.5	3.68	604.19	57.83
	5	3.46	604.19	57.83
	10	3.19	618.21	58.42
480	0.1	4.35	746.04	57.24
	0.5	3.90	730.34	56.69
	1.5	3.71	730.34	56.69
	5	3.19	730.34	56.69
	10	3.20	746.04	57.24

The results indicate that increasing of the opening depth can reduce the values of maximum subsidence (Figures 3.6 and 3.7) and properties of roof thickness, while increasing of the elastic values of roof thickness tends to decrease the maximum subsidence. The trough widths increase and  $S_{\max}$  decreases with increasing opening depth. They reach a constant when the D/H ratios are greater than 30. This complies with the postulation given by Singh (1992) which suggests that under critical and sub-critical subsidence the angles of draw and the maximum subsidence are sensitive to height and depth of shallow opening. They are not sensitive to opening at great depth.

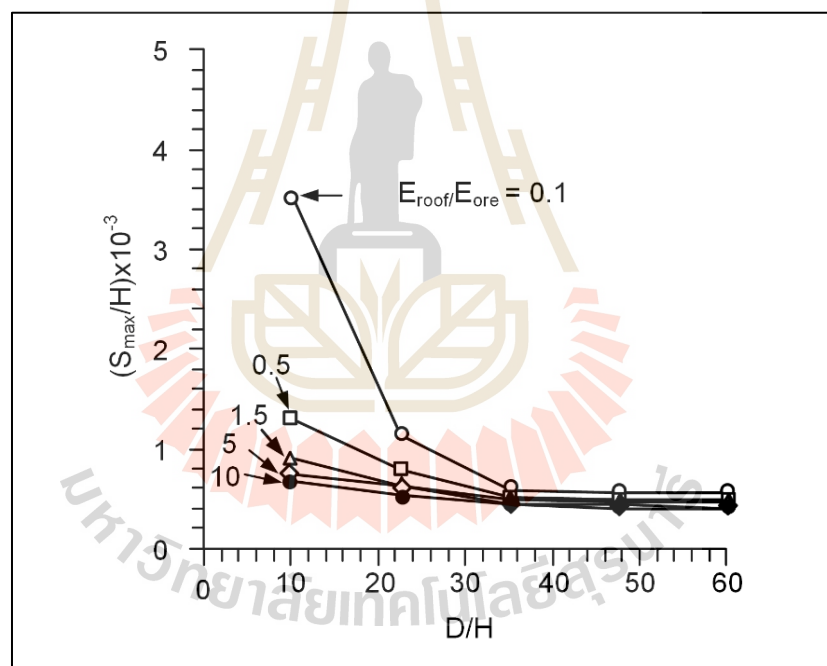


**Figure 3.6** Normalized subsidence vs normalize opening depth

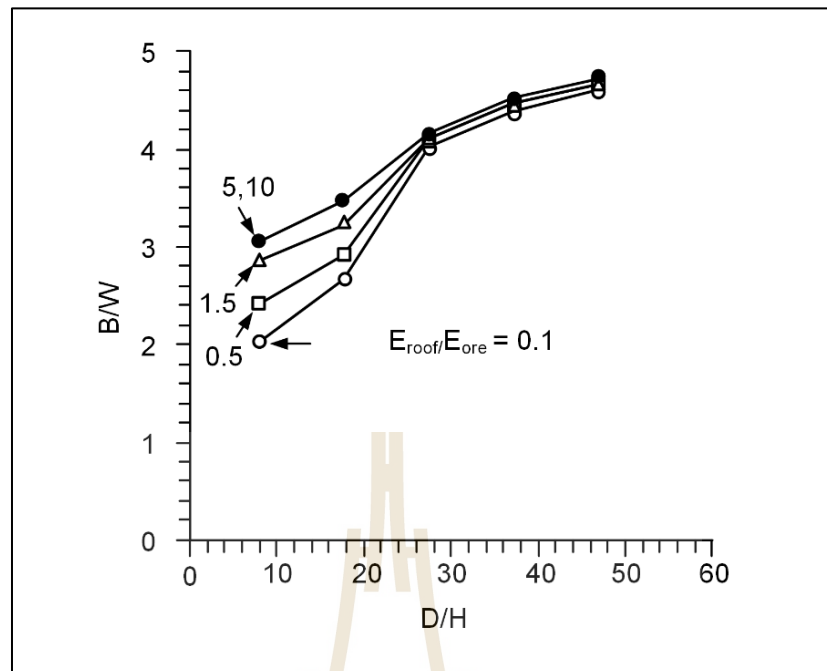


**Figure 3.7** Normalized limit trough wide vs of normalize opening depth

## CHAPTER IV

### PHYSICAL MODEL SIMULATIONS

#### 4.1 Introduction

The physical model simulations are carried out to determine the effects of overburden properties and roof thickness on the maximum subsidence and trough width under sub-critical subsidence.

#### 4.2 Material property

The main factor of the selection of synthetic gel used to simulate the overburden is universally obtainable and non-toxic. The properties of the overburden should be independent of the variations of temperatures and humidity.



**Figure 4.1** Synthetic gel mixed with paraffin under 60 °C planed in oven

First, the mechanical properties of the gel are determined by performing uniaxial compression test. Figure 4.1 shows the synthetic gel mixed with paraffin wax under constant temperature of 60 °C in the oven and then poured into the PVC pipe with size of 25.4 mm length and 12.5 mm diameter. After cooling down to 32 °C, the gel becomes semi-solid specimen (Figure 4.2).

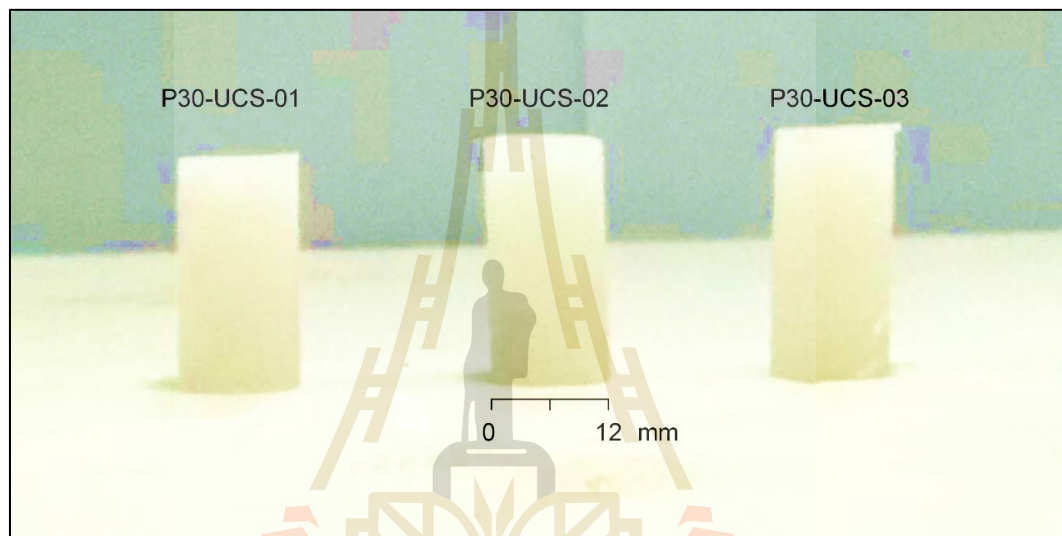


**Figure 4.2** Gel specimens prepared for uniaxial test

Based on Sartkaew et al. (2016), the synthetic gel to paraffin wax ratios is selected as 70:30 by weight. The uniaxial compression test is carried out to identify the elastic modulus and Poisson's ratio of the gel by using universal testing machine (UTM) (Figure 4.3). The test method follows the ASTM standard practice (ASTM D695-10, 2010). Table 4.1 summarizes dimensions, volume and density of the specimen. The average density of gel specimens is 0.86 g/cm<sup>3</sup>. Figure 4.4 shows the stress-strain curves obtained from the testing. From the unloading curves, the elastic modulus is 2.20 ± 0.38 MPa and Poisson's ratio is 0.36. The density of 0.86 ± 0.01g/cm<sup>3</sup>.

Sartkaew et al. (2016) state that the elasticity of gels increasing exponentially with the paraffin additive. Poisson's ratios are however not sensitive to the paraffin content.

**Table 4.1** Specimen dimensions prepared for uniaxial compression testing.

Specimen No.	Weight (g)	Diameter (mm)	Height (mm)	Volume (cm <sup>3</sup> )	Density (g/cm <sup>3</sup> )
P30-UCS-01	171.98	51.22	96.36	198.45	0.87
P30-UCS-02	181.30	52.18	97.20	207.75	0.87
P30-UCS-03	140.28	51.56	79.20	165.28	0.85
Average					0.86 ± 0.01



**Figure 4.3** Gel specimen placed in a universal testing machine (UTM)

### 4.3 Design and fabrication of test apparatus

The functional requirements for the test frame are to simulate and measure the model subsidence of overburden under real gravitational force in three-dimension and to assess the effect of overburden properties on subsidence trough.

The apparatus (Figure 4.5) comprises three main components: material container, mine opening simulator and surface measurement system. The opening simulator is an array of plastic blocks with size of 25 mm length, 70 mm wide and 25 mm high. These blocks simulate the opening in the center of the material container. After the synthetic gel is installed with defined overburden thickness, these blocks are gradually moved out, and hence induces the vertical settlement of the gel above.

The measurement system is a sliding rail with laser scanner. The laser scanner can be moved horizontally in two perpendicular direction. The precision of the measurements is one micron. The trough profile are recoded and plotted in two dimensional profiles. The angles of draw, slopes and maximum subsidence values of the subsidence trough are measured.

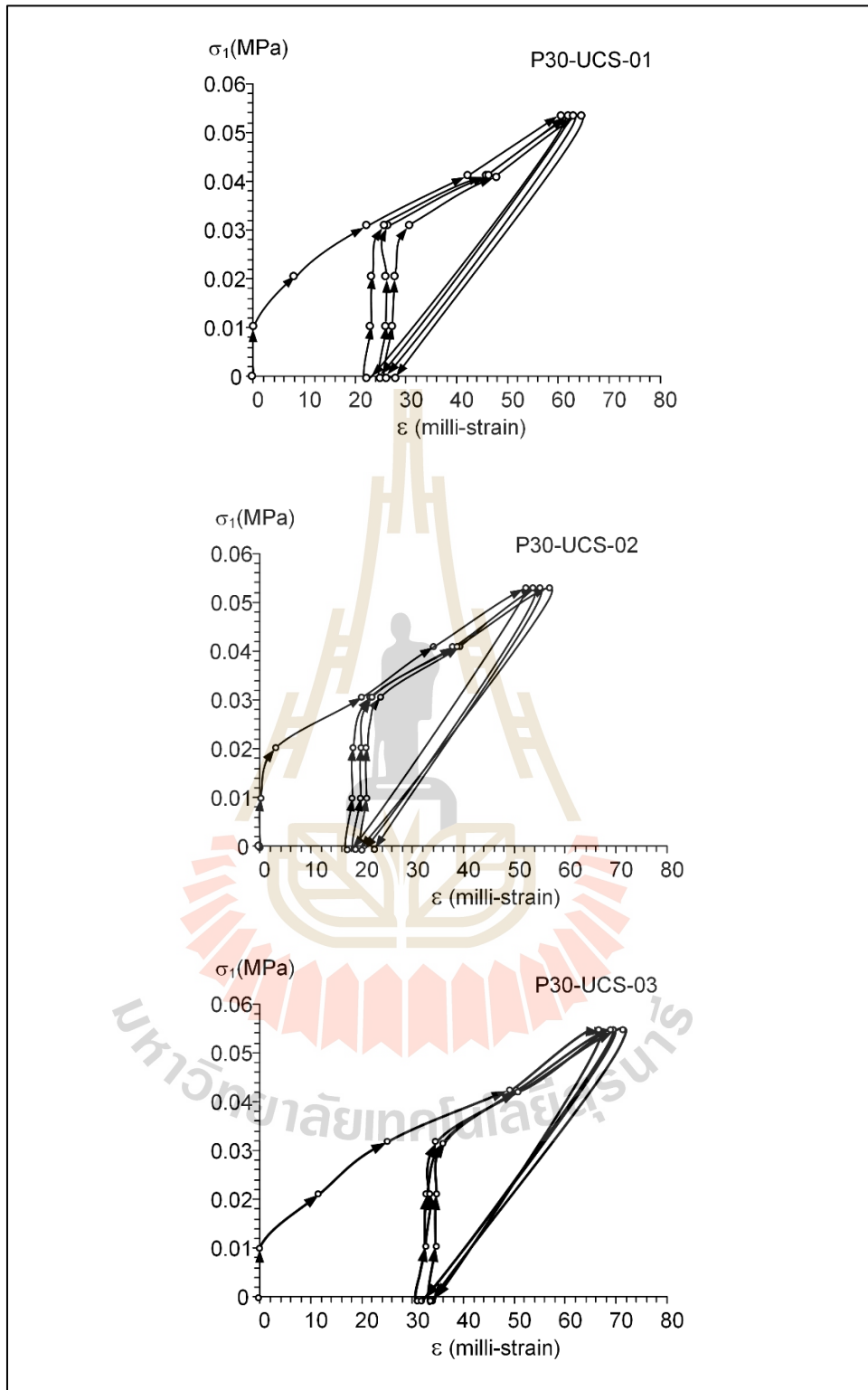


**Figure 4.4** Stress-strain curves obtained from gel specimens with paraffin contents 30%

by weight



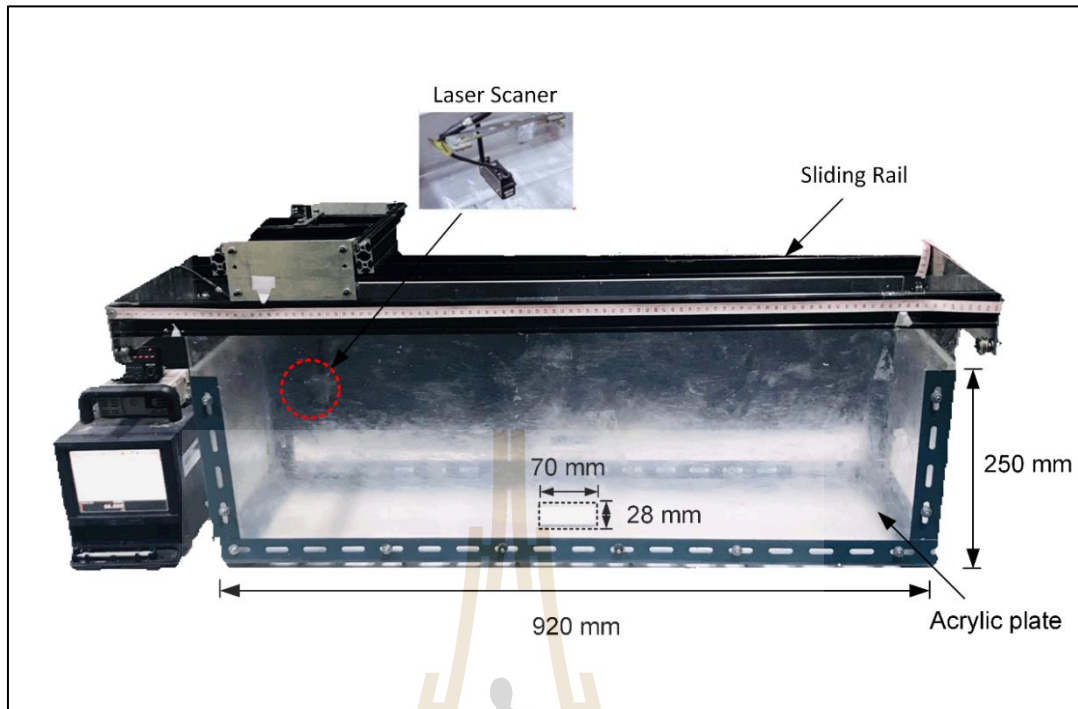


**Figure 4.5** Apparatus used for physical model testing

#### 4.4 Physical model simulations

Physical model simulations have been performed to determine the effects of opening roof thickness and properties of overburden on surface subsidence under sub-critical condition. The subsidence components considered here include angle of draw, maximum subsidence and trough width. A model apparatus is used to represent the three-dimensional simulations of surface subsidence which allows fully controlled test conditions (Figure 4.6). The roof thickness ( $t$ ) is varied from 14, 21, 28, 35 to 42 mm,  $t/W$  ratios are 0.2, 0.3, 0.4, 0.5 and 0.6. The opening width ( $W$ ), height ( $H$ ) and length ( $L$ ) are maintained constant at 70, 28 and 250 mm, respectively. The elastic moduli of roof thickness are  $2.20 \pm 0.38$  MPa and density  $860 \pm 1$  kg/m<sup>3</sup>. The plastic blocks equivalent to the predefined  $W$ ,  $H$  and  $L$  are placed in the material container. For each series of

simulation the synthetic gel are melted to obtain viscous fluid under the temperature of 60 °C (Figure 4.7). It is poured in the container to a pre-defined thickness (Figure 4.8). The thickness of the synthetic gel layer represents the roof thickness. After the synthetic gel becomes semi-solid under temperature of 32 °C, the blocks are gradually and systematically moved down, and hence induces the vertical settlement of the synthetic. The laser scanner is used to measures the surface trough profile before and after the subsidence is induced. The results are recorded and plotted in two-dimensional profiles. The subsidence profiles are used to calculated the subsidence components including the angle of draw, maximum subsidence and limit trough width.

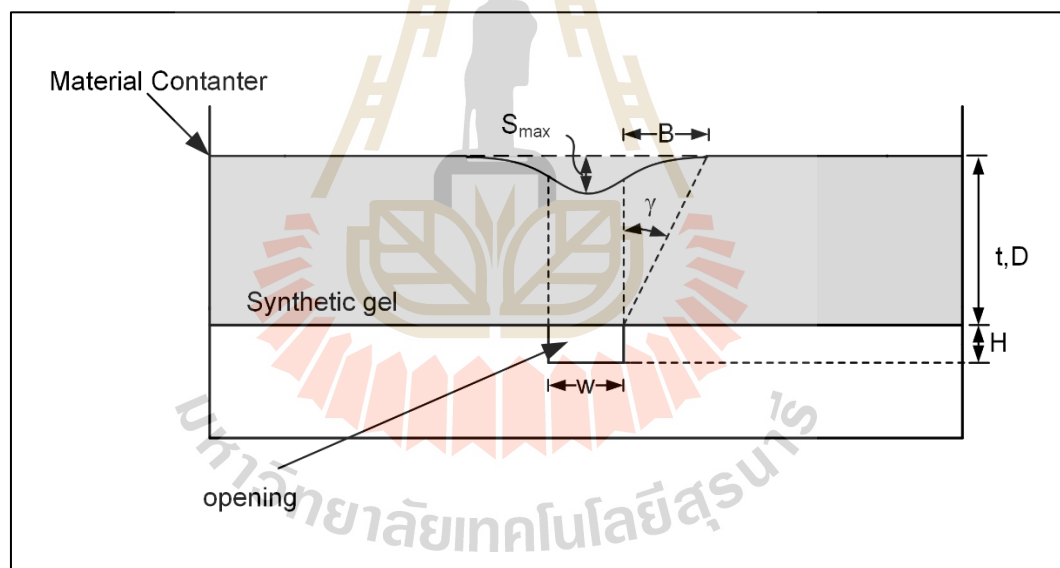


**Figure 4.6** Variable used in simulations



**Figure 4.7** (a) Synthetic gel (b) Synthetic gel melted into viscous fluid under temperature of 60 °C

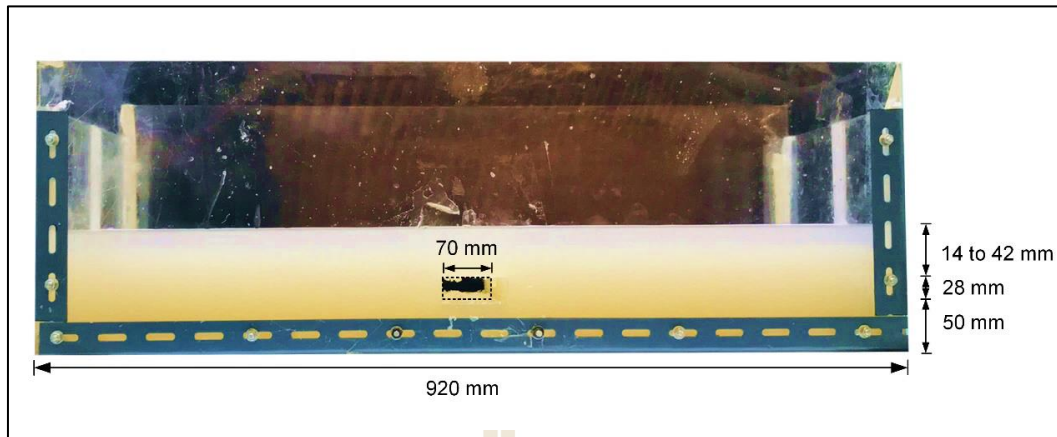


**Figure 4.8** Filling synthetic gel into material container with pre-defined thickness

#### 4.5 Test results

The measurement results obtained here are shown in Table 4.2. The  $S_{\max}$  (Figure 4.9) and  $B$  (Figure 4.10) are plotted as a function of opening roof-to-opening width ( $t/W$ ) ratios for each opening width ( $W$ ). The results show that the  $S_{\max}$  decreases with increasing opening roof. The maximum subsidence reaches constant where roof thickness at  $t/W$  ratios are greater than 0.4. This is because the elastic modulus of the roof above opening is constant for all conditions and the subsidence is not affected when roof is sufficiently thick. The trough width increases with increasing opening roof. This is because under sub-critical conditions, the maximum subsidence decreases with increasing trough widths (Singh, 1992).

The test results in Figures 4.9 and 4.10 indicate that the decrease of maximum subsidence is related to the increase of roof thickness, while the increase of trough width are related to the increase of opening roof. The maximum subsidence is constant, when the opening roof-to-opening width ratios are greater than 0.4.

#### 4.6 Comparison of computer and physical model simulations

The physical test results are compared with those observed from the finite difference analysis by using Phase 2.8 under properties and boundary of physical models, as shown in Figure 4.11 for various opening roofs. The results show that the subsidence profiles obtained from the numerical model that is shallower and narrower than obtained from those physical model. This is probably due to number and sizes of elements used in the mesh model. The larger number of the elements and smaller elements would provide even closer of the computer model to the physical model test results.

**Table 4.2** Physical model test variables and results

Test variables			Results		
No.	Opening roof to-opening width ratio $t/w$	Roof thickness $t_r$ (mm)	$S_{max}$ (mm)	B (mm)	$\gamma$ (degrees)
1	0.2	14	7.32	85	71.77
2	0.3	21	5.83	105	75.07
3	0.4	28	5.22	125	77.37
4	0.5	35	4.92	125	77.37
5	0.6	42	4.89	125	77.37

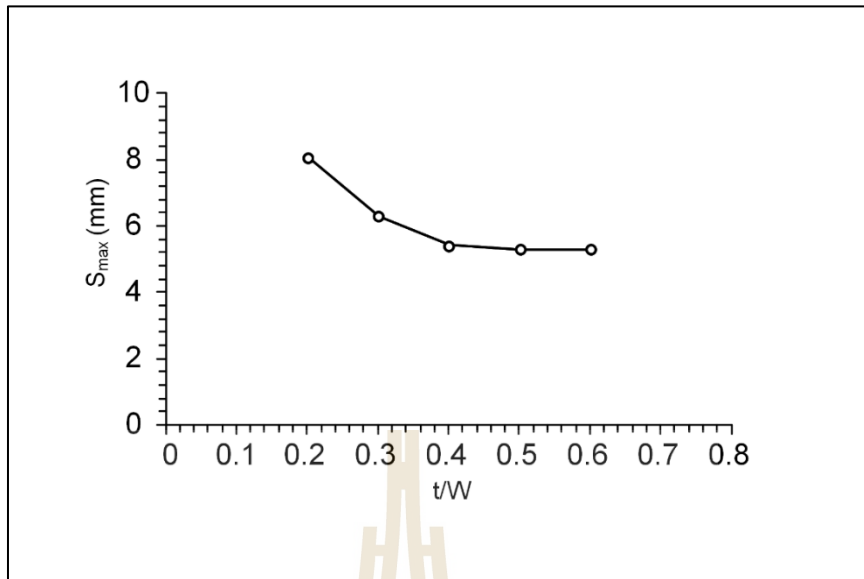


**Figure 4.9** Maximum subsidence ( $S_{\max}$ ) as a function of opening roof-to-opening width ratios ( $t/W$ )

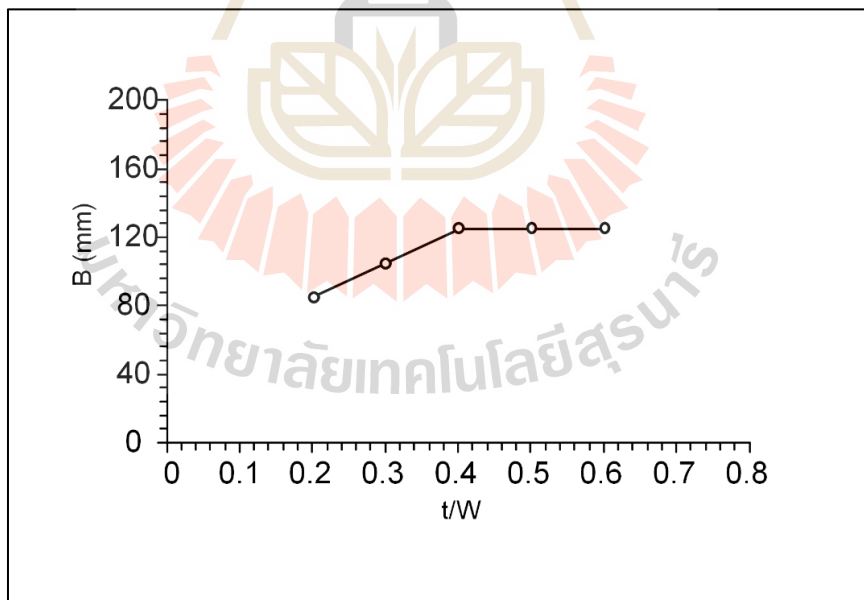


**Figure 4.10** Trough wide (B) as a function of opening roof-to-opening width ratios ( $t/W$ )

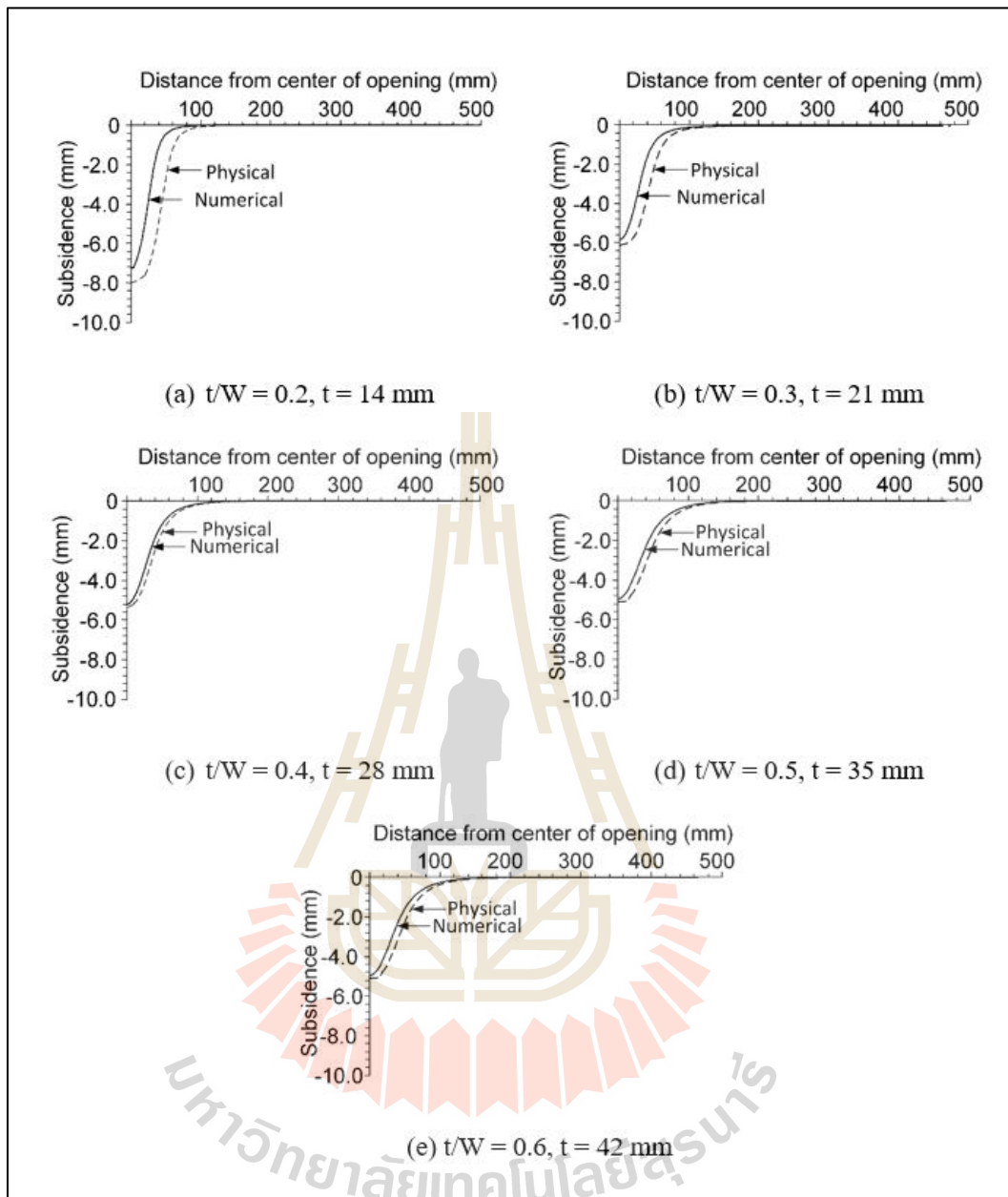


**Figure 4.11** Comparisons of subsidence profiles measured from physical and predicted by numerical model under various opening roof.

## CHAPTER V

### DISCUSSIONS AND CONCLUSIONS

#### 5.1 Discussions

Comparisons of the findings and results from this study with those obtained elsewhere under similar test conditions are made.

1) Phase 2.8 simulation results agree well with the measurements from the physical modelling, suggesting that the test results are sufficiently reliable. The agreement between the numerical simulations and the physical model tests suggests that the concept, procedure and results in the numerical simulation are appropriated and correct. The results obtained from both methods indicate that maximum subsidence decreases with increasing opening roof thickness. The maximum subsidence reaches constant where roof thickness under  $t/W$  ratios are greater than 0.4.

2) The surface subsidence profiles measured from the numerical model are shallower and narrower than those obtained from the physical model. Under the same opening geometry, a soft roof thickness (lower  $E_{\text{roof}}$ ) shows deeper subsidence trough and narrower extent than those obtained under stiffer overburden (higher  $E_{\text{roof}}$ ). The observation agrees reasonably well with those found by Yao et al. (1991) and Sartkaew et al. (2016)

3) Numerical and physical simulations are applicable for the horizontal bedding, when the stiffness of roof thickness is greater than the overburden. Noted that the results obtained here are simulated under single opening condition, the effect of inclined bedding and mining with room-and-pillar-method are not considered in this



study. The results clearly show that under sub-critical subsidence, the angles of draw and maximum subsidence are sensitive to height and depth of shallow opening. This agrees with Singh (1992).

## 5.2 Conclusions

Physical models have been performed to simulate surface subsidence of overburden in 3-dimensions. The opening height (H) and width (W) are 25 and 70 mm for all tests. The results of the numerical and physical simulations can be concluded as follows:

1) The effects of roof thickness can be observed from relationship between  $S_{\max}/H$  and  $t/W$  ratios. The results show that  $S_{\max}/H$  ratios decrease with increasing roof thickness. The maximum subsidence reaches constant where the  $t/W$  ratios are equal to or greater than 0.4. This makes the subsequent numerical simulations much more simple.

2) Under the same opening depth and width, a soft roof thickness (lower  $E_{\text{roof}}$ ) causes maximum subsidence to increase and limit trough width extents decrease more than those obtained under stiffer roof thickness (higher  $E_{\text{roof}}$ ). This is primarily because soft overburden can deform easier than rigid overburden.

3) The increasing of opening depth and elastic modulus of roof above the opening can reduce of the maximum subsidence values.

## 5.3 Recommendations for future studies

To further verify the conclusions drawn in this research, more testing is required as follows:

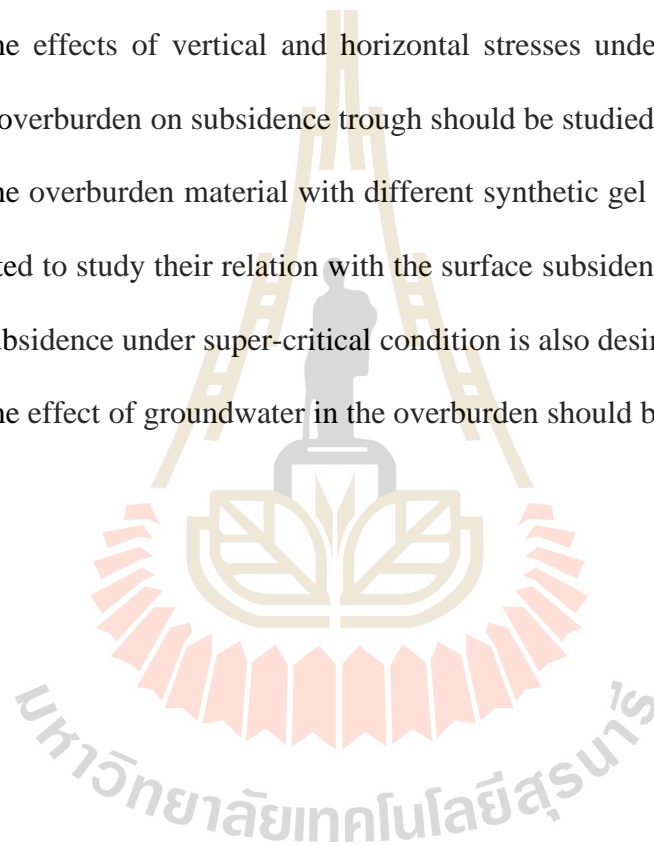
1) The physical model simulations should be performed on a wider range of the opening geometries to confirm the effects of opening depth, and width on of surface subsidence extent. More testing is also preferable on a variety of materials with different mechanical properties of overburden simulations.

2) The effect of topography and inclination of overburden should also be studied.

3) The effects of vertical and horizontal stresses under various mechanical properties of overburden on subsidence trough should be studied.

4) The overburden material with different synthetic gel to paraffin wax ratios should be tested to study their relation with the surface subsidence. The knowledge of the surface subsidence under super-critical condition is also desirable.

5) The effect of groundwater in the overburden should be studied.

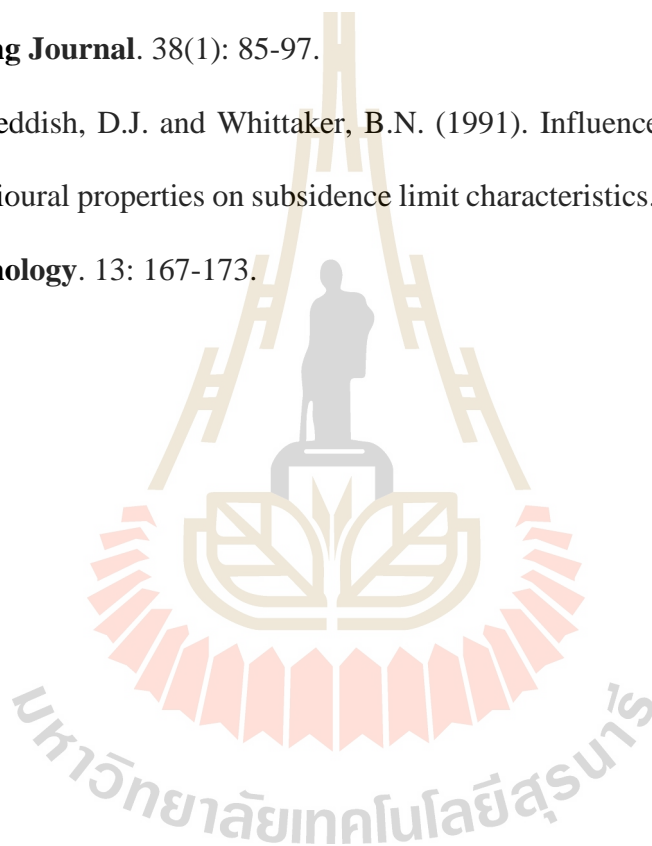


## References

- Aracheeploha, S., Horkaew, P., and Fuenkajorn, K. (2009). Prediction of cavern configurations from subsidence data. **In Proceedings of the Second Thailand Symposium on Rock Mechanics**. Suranaree University of Technology, Thailand. pp. 116-176.
- Asadi, A., Shahriar, K., Goshtasbi, K., and Najm, K. (2005). Development of new mathematical model for prediction of surface subsidence due to inclined coal-seam mining. **Journal of the Southern African Institute of Mining and Metallurgy**. 105: 15-20.
- ASTM D695-10 (2010). **Standard test method for compressive properties of rigid plastics**. Annual Book of ASTM Standards, American Society for Testing and Materials, West Conshohocken, PA.
- Crosby, K.S. (2007). Integration of rock mechanics and geology when designing the Udon South sylvinitic mine. **In Proceeding of the 1th Thailand Symposium on Rock Mechanics**. (pp. 3-22).
- Itasca (2001). **User Manual for Phase<sup>2</sup> Langrangian Analysis of Continua**. Version 8.0, Minneapolis, Minnesota.
- Jiang, M. and Yin, X. (2014). Influence of soil conditioning on ground deformation during longitudinal tunneling. **Comptes Rendus Mecanique**. 342: 189-197.

- Park, D. and Li, J. (2004). Subsidence simulation using laser optical triangulation distance measurement devices. **In Gulf Rocks 2004, the Sixth North America Rock Mechanics Symposium**. Houston, Texas.
- Ren, G. and Li, J. (2008). A study of angle of draw in mining subsidence using numerical modeling techniques. **Electronic Journal of Geotechnical Engineering**. 13: 1-14.
- Saoanunt, N. and Fuenkajorn, K. (2015). Physical model simulations of super-critical subsidence as affected by mining sequence and excavation rate. **In Ninth South East Asia Technical University Consortium Symposium**, Suranaree University of Technology, Thailand. pp. 22-25.
- Sartkeaw, S. and Fuenkajorn, K. (2016). Verifications of empirical method and numerical simulation using physical model for subsidence prediction of Maha Sarakham formation. **Research and Development Journal of the Engineering Institute of Thailand under H.M. the King's Patronage**. 27(3): 17-24.
- Singh, M.M. (1992). Mine subsidence. In H.L. Hartman (ed). **SME Mining Engineering Handbook**. society for mining metallurgy and exploration. littleton, colorado. pp. 938-971.
- Terzaghi, K. (1936). Stress distribution in dry and in saturated sand above a yielding trap-door. **In Proceedings of the International Conference on Soil Mechanics**, Harvard University. Press, Cambridge, Massachusetts. 1:307-311.
- Thongprapha, T., Fuenkajorn, K., and Daemen, J.J.K. (2015). Study of surface subsidence above an underground opening using a trap door apparatus. **Tunnelling and Underground Space Technology**. 46: 94-103.

- Tunsakul, J., Jongpradist, P., Kongkitkul, W., Wonglert, A., and Youwai, S. (2013). Investigation of failure behavior of continuous rock mass around cavern under high internal pressure. **Tunneling and Underground Space Technology**. 34: 110-123.
- Wang, F., Du, Y.J., and Yang, X. (2015). Physical modeling on ground responses to tunneling in sand considering the existence of HDPE pipes. **Geotechnical Testing Journal**. 38(1): 85-97.
- Yao, X.L., Reddish, D.J. and Whittaker, B.N. (1991). Influence of overburden mass behavioural properties on subsidence limit characteristics. **Mining Science and Technology**. 13: 167-173.



## **BIOGRAPHY**

Miss Pattarapon Roekyindee was born on December 26, 1994 in Bangkok, Thailand. She received her Bachelor's Degree in Engineering (Geological Engineering) from Suranaree University of Technology in 2017 and received her Master's Degree in Civil, Transportation and Geo-resources Engineering Program, Institute of Engineering, Suranaree University of Technology. During graduation, 2017-2019, she was a part time worker in position of research assistant at the Geomechanics Research Unit, Institute of Engineering, Suranaree University of Technology.

